Tailoring Wettability to Push the Limits of Condensation

Jianxing Sun[a,b], Patricia B. Weisensee[b,c,*]

a. Department of Materials Science and Engineering, University of Michigan, Ann Arbor, USA

b. Department of Mechanical Engineering & Materials Science, Washington University in St. Louis, USA

c. Institute of Materials Science and Engineering, Washington University in St. Louis, USA

* Corresponding author: p.weisensee@wustl.edu

Abstract

Wetting plays a crucial role in achieving efficient condensation in applications such as atmospheric water harvesting, air conditioning and refrigeration, and thermal power plants. Despite decades of research, the industrial implementation of dropwise condensation, which is often superior to filmwise condensation, has been limited, mostly due to the poor durability of promoter coatings and the challenge of achieving dropwise condensation for non-aqueous working fluids. Both areas have seen noteworthy advancements over the past few years, some of which we highlight in this review article. For example, recognizing that contact angle hysteresis, not contact angles per se, are responsible for enabling dropwise condensation, ultra-smooth liquid-like polymer coatings and lubricant-infused surfaces were developed for use with water and non-aqueous working fluids. There are also several new developments for passive and active droplet removal. Advances in coating durability include a better understanding in the failure mechanisms and physics-informed designs of new coating processes and chemistries.

Keywords

Dropwise condensation, Contact angle hysteresis, Non-aqueous working fluids, Lubricant-infused surfaces, De-wetting transition, Passive droplet removal

1. Introduction

Condensation, a phase change process in which vapor turns into liquid, is ubiquitous both in nature and technological applications, ranging from the formation of rain droplets [1] to atmospheric water harvesting [2] and to steam condensers in large thermal power plants [3,4]. The ability to tailor surface wettabilities – and with that droplet mobilities – over multiple length scales has proven crucial to controlling droplet nucleation, droplet growth, and droplet removal, all of which are important to achieve and sustain an efficient condensation process. Particularly the rapid advancement of micro/nano fabrication techniques over the past two decades has pushed condensation heat transfer rates to ever higher limits [5]. Figure 1 compares various recent surface and coating designs based on their wettability (characterized by the contact angle, CA) and liquid mobility (characterized by the contact angle hysteresis, CAH), and differentiates between different modes of condensation. More information on CA and CAH is provided in section 2.1.

Irrespective of the type of the surface, droplets first must form *via* heterogeneous nucleation. The kinetics, or "effectiveness", of the nucleation and subsequent droplet growth processes are highly dependent on the wettability of the respective surface [6]. Droplets nucleate more easily on surfaces with high wettability (low CAs) and high conformity (soft or liquid surfaces) [7]. On these surfaces, droplet mobility is typically limited (high CAH, Regime I in Fig. 1), leading to the formation of a continuous liquid film that covers the entire surface as condensation progresses. This mode of condensation is known as filmwise condensation (FWC) and is the most common naturally occurring condensation mode. During condensation of pure vapor, this film acts as a strong thermal resistance, significantly restricting the heat transfer between the warm vapor and the cold substrate. Preventing film formation or disrupting the condensate layer has thus been central to many research efforts [8–10] (for a recent review article on FWC-enhancement, we would like to refer the reader to ref. [11]). On the contrary, for condensation of moist air, *i.e.* condensation in the presence of non-condensable gases (NCGs), the gas diffusion layer presents the stronger resistance and FWC with its enhanced nucleation rates and simple surface design can be beneficial, as recently confirmed by Thomas *et al*. [12].

Opposite to FWC, in dropwise condensation (DWC) on non-wetting surfaces (intermediate or high CAs, small to intermediate CAH, Regimes II & III in Fig. 1), nucleation is delayed, however, condensing droplets have a high enough mobility to depart the surface before coalescing into a film, clearing the surface for frequent re-nucleation and fast droplet growth. Schmidt and co-workers [13] reported in their seminal work from 1930 a 5-12-fold increase in the vapor-side heat transfer coefficient (HTC) for DWC as compared to FWC (2-3x global HTC enhancement). Since then, extensive research efforts have been devoted to 1) better understanding the mechanisms and predicting the heat transfer performance of DWC (for a recent summary on theory and modeling of DWC, see [14]), 2) discovering new/different modes of DWC and heat transfer enhancements, and 3) improving the design and functionality of surface coatings. For excellent in-depths reviews of different surface designs that promote DWC, we would like to refer the reader to refs. [15] and [16].

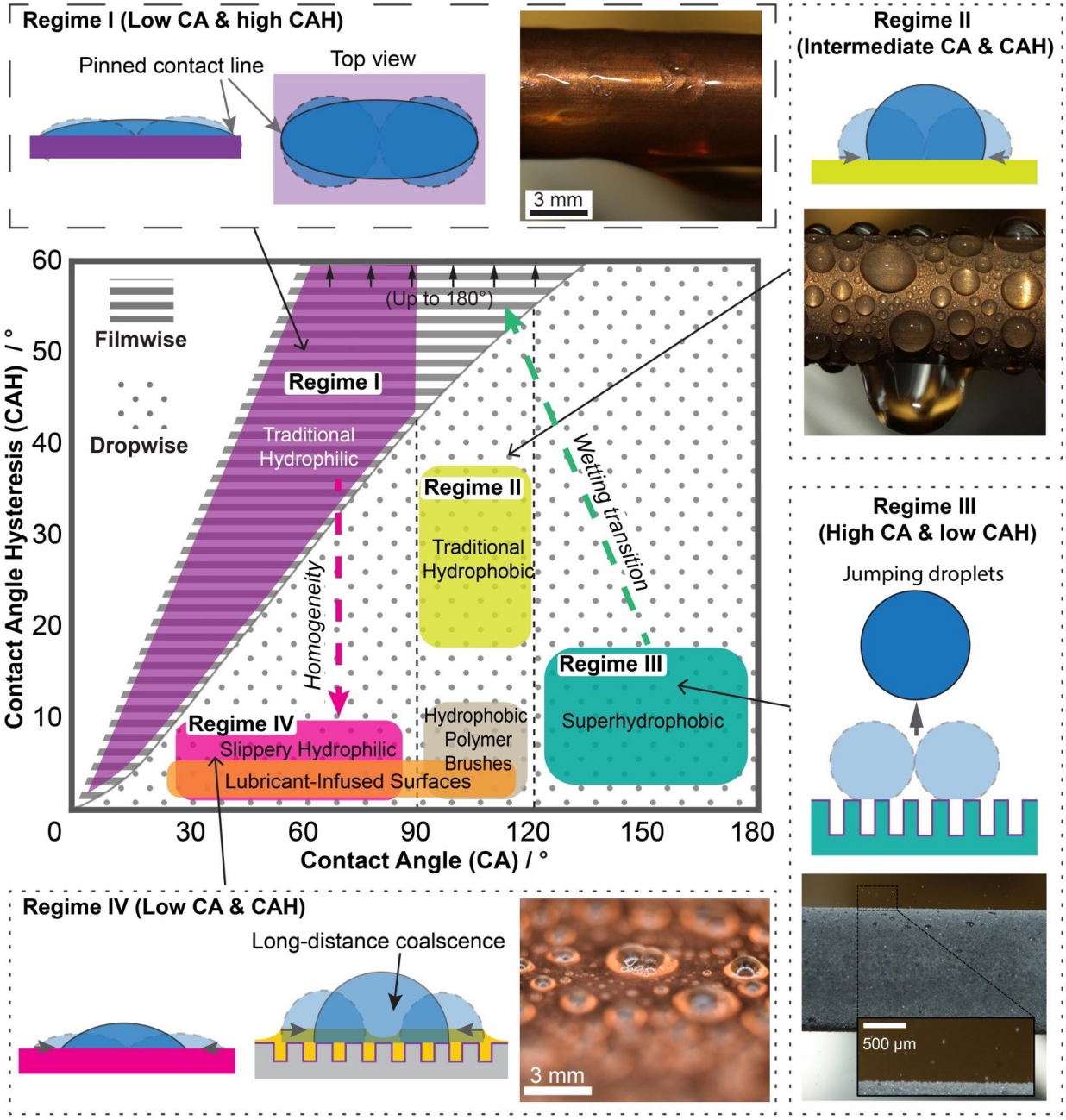

Figure 1: Overview of condensation modes on different coatings with distinctive contact angles (CA) and contact angle hysteresis (CAH). Contact line dynamics during coalescence influence the mode of condensation on different coatings, which can be categorized into four regimes based on the combination of CA and CAH. The experimental images are from ref. [17].

For many years, the biggest hinderances to the commercial implementation of DWC were the low long-term durability of most promoter coatings [18] and the challenge of promoting DWC for non-aqueous working fluids [19]. Both areas have recently seen noteworthy advancements. In this perspective, we will focus primarily on a few select developments during the past two to three years, rather than providing a comprehensive review, highlighting the most recent advances on coating development and condensate removal strategies in the context of surface wettability and condensate

mobility, and provide our perspectives on current and future challenges in the field of condensation heat transfer on external surfaces.

2. Droplet wettability and mobility in condensation heat transfer

2.1. Contact angles and contact angle hysteresis of sessile droplets

A key to effectively managing the condensation process are the surface wettability and condensate mobility. Wettability is typically characterized using the contact angle θ between the gas (or vapor) phase, the liquid droplet, and the solid substrate. On a chemically and structurally homogeneous rigid surface, the static (*i.e.*, equilibrium) contact angle is described by Young's law:

$$\cos\theta_{\mathrm{Y}} = \frac{\gamma_{\mathrm{sv}} - \gamma_{\mathrm{sl}}}{\gamma_{\mathrm{lv}}}, \qquad (1)$$

where γ_{sv}, γ_{sl}, and γ_{lv} are the solid-vapor, solid-liquid, and liquid-vapor interfacial energies, respectively. Clean surfaces of common heat transfer materials, such as metals, have high surface energies and are hence (hydro-)philic, resulting in water (and other working fluids) to form a liquid lens or film featuring a contact angle $\theta_{\mathrm{Y}} < 90°$, similar to the droplet shown in the "Regime I"-box in Fig. 1. These materials can be transformed into hydrophobic surfaces by applying a low-surface-energy promoter coating, featuring water contact angles on a smooth surface in the range of 90° to 120°. To achieve even higher contact angles, such as those on a superhydrophobic surface with an apparent contact angle $\theta^* \geq 150°$, nano- and/or micro-scale surface features need to be added, such that the droplet sits on a composite surface of solid structures and air pockets, which is often referred to as the Cassie-Baxter (C-B) state. It is important to note, though, that the apparent contact angle represents the macroscopic droplet geometry; locally, the liquid contacts the solid at, or close to, its equilibrium contact angle $\theta_{\mathrm{Y}} \leq 120°$ [20]. For rough surfaces with an intrinsic contact angle $\theta_{\mathrm{Y}} < 90°$, the liquid will typically penetrate the asperities (except for surfaces with sophisticated re-entrant geometries), resulting in a highly wetting Wenzel state.

In condensation heat transfer, as we will discuss in more detail in the following section, the mobility of the droplet is more important than the wettability. Droplet mobility is traditionally quantified using the contact angle hysteresis (CAH), $\Delta\theta = \theta_{\mathrm{A}} - \theta_{\mathrm{R}}$, which is the difference between the contact angles at the advancing (A) and receding (R) sections of the droplet as its contact line (CL) slowly moves across the surface. The smaller the CAH, the lower the resistance from CL pinning and the higher the droplet mobility. Unless great care is taken to fabricate high-quality surfaces, in most situations, CAH is high due to pinning of the receding contact line at topographical or chemical defects [21].

2.2. The role of contact angles and contact angle hysteresis on (dropwise) condensation

Condensation, and especially DWC, is a cyclic process, in which droplets nucleate on the surface, grow through direct condensation and coalescence, and eventually shed from the surface due to gravity. While the contact angle dictates the nucleation kinetics [22,23], the dynamics of the contact line and the mobility of the droplets determine the mode of condensation [24]. Despite early indications that the contact angle hysteresis, not contact angle per-se, determines whether condensation occurs in the

filmwise or dropwise mode [25], many researchers have focused on optimizing (static) contact angles during the development of new coatings. When the CAH is high, the released surface energy upon coalescence of two droplets (~ γ ~ CA) is not sufficient to overcome contact line pinning (*i.e.*, viscous dissipation at the contact line, ~ CAH), irrespective of the droplet's CA. The droplet is "stuck in place", as shown in the "Regime I"-box in Fig. 1. Consequently, after multiple coalescence events, DWC transitions to FWC due to the inability to remove individual droplets. Chu *et al.* [26] defined a *Hysteresis number* = sin(*CAH*/2)/tan(*CA*/2) and introduced four regions that represent different combinations of CA and CAH, similar to our four regimes shown in Fig. 1. Only droplets in the regimes with relatively low CAH are able to fully relax and form circular contact lines upon coalescence (see boxes for Regimes II-IV in Fig. 1) – a prerequisite for DWC. Chu and co-workers did not conduct experiments for Regime IV (low CA, low CAH) droplets and identified only one example of DWC for such droplets – that of water condensation on a lubricant-infused surface ($\theta \approx 65°$, $\Delta\theta < 3°$) [27], though in recent years there have been many more examples of water condensation on lubricant-infused surfaces, as we will discuss in more detail in section 2.4.

Cha *et al.* [28] were the first to demonstrate DWC of Regime IV water droplets on solid hydrophilic surfaces and confirmed that CAH, rather than the CA, is indeed the decisive variable for DWC. They prepared a novel solid hydrophilic PEGylated silicon surface ($\theta_A = 38°$), which, due to its sub-nanoscale roughness and supreme chemical homogeneity, had an extremely low CAH (<3°), leading to efficient droplet shedding and consequently dropwise condensation. Nakamura *et al.* [29] found that the CA (and CAH) of the samples are significantly influenced by both the PEG chain length (best for droplet sliding: n = 9-12) and the mixing ratio of PEG_n-Si and tetraethoxysilane. Furthermore, Kota *et al*. [30] systematically elucidated the design of slippery hydrophilic (SLIC) surfaces by covalently grafting polyethylene glycol brushes to silicon substrates. The level of slipperiness was found to increase with increasing grafting density, since water molecules can penetrate the gaps between PEG brushes at a low grafting density and increase pinning and resistance forces of water droplets. A plateau in slipperiness is expected at a critical grafting density, where the brush size is equal to the inter-tether distance. SLIC surfaces are ideal for dropwise condensation owing to their low static contact angle and low contact angle hysteresis. The low CA can promote high nucleation rates and results in a low conduction resistance through the droplet and a larger liquid-solid contact area, which are all beneficial for condensation heat transfer [31]. The low CAH can efficiently remove condensed droplets, maintaining the dropwise mode. One potential downside of these surfaces is their need for extremely smooth substrates, such as silicon wafers or glass coverslips, possibly limiting their applicability in industrial applications.

Surfaces in Regimes II and III (intermediate to high CA, low to intermediate CAH) are more commonly used for DWC. They are typical of high-quality smooth hydrophobic and superhydrophobic surfaces. Similar to Regime IV surfaces, the CL can easily relax upon droplet coalescence, forming a new droplet with larger volume, which can eventually be removed from the surface by gravity or other removal mechanisms (different condensate removal strategies will be discussed in more detail in section 4). For example, Monga *et al*. [32] showed that shorter, flexible polymer brushes of smooth hydrophobic

quasi-liquid surfaces result in higher water condensation rates than longer polymer chains (this is in contrast to Nakamura's findings discussed above), which easily get entangled and increase surface roughness and CAH. On superhydrophobic surfaces with extremely high CA, the small solid-liquid contact area not only minimizes (lateral) CL pinning (with CAH similar to high-quality smooth hydrophobic surfaces), but also provides very little adhesion perpendicular to the solid surface [33]. Excess kinetic energy released from the coalescence of two droplets can self-propel the merged droplets across the surface [34] or cause them to jump off the surface, as illustrated in the "Regime III"-box in Fig. 1 [17,35]. The size of jumping droplets is typically on the order of 10s of μm, signifying extremely efficient droplet removal that can significantly enhance condensation heat transfer rates [17,36]. Through careful surface design, jumping droplets can even be as small as ~1 μm in diameter, with a further decrease in size inhibited by viscous dissipation during the coalescence process, even in the case of ideal surface wettability [37]. For more information on jumping droplet heat transfer, we refer readers to a recent review article that discusses the requirements, mechanisms, and drawbacks of superhydrophobic surfaces that promote droplet jumping [38].

2.3. Ultra-smooth coatings for dropwise condensation of non-aqueous working fluids

Due to their low surface tension, non-aqueous working fluids, such as alkanes, alcohols, and fluorocarbons always have static or advancing contact angles significantly less than 90° on non-structured hydrophobic surfaces, as shown in Fig. 2a, and very often receding contact angles of zero. Figure 2b shows that droplets with relatively high CAH have an elongated geometry upon droplet sliding. Consequently, these low-surface tension fluids usually condense in a filmwise mode on convectional hydrophobic and superhydrophobic surfaces, as shown in Fig. 2c. However, similar to the ability of slippery hydrophilic surfaces discussed in the previous section to promote DWC of water, ultra-smooth grafted polymer surfaces are also able to promote DWC of many non-aqueous working fluids. Khalil *et al*. [39] demonstrated sustained DWC of ethanol, hexane, and pentane on initiated chemical vapor deposited (iCVD) surfaces and measured a 4- to 8-fold enhancement in the vapor-side HTC, whereby initiator-grafted polymers had a 1.5x-2x higher HTC than silane-grafted coatings. The authors also demonstrated DWC of these non-aqueous working fluids on iCVD-coated titanium surfaces, which have a higher roughness than silicon wafers and hence present a more realistic scenario for use in industrial condensers. Rabbi and co-workers [40] showed that brush-like siloxane-silane coatings on copper and aluminum tubes enable DWC for ethanol, hexane, and pentane for at least 15 days, with up to 640% heat transfer enhancements. Soltani and Golovin [41] demonstrated DWC of n-decane on liquid-like brushes made from polydimethylsiloxane (PDMS) and perfluoroether (PFPE). Both surfaces exhibit ultra-low CAH (< 2°), whereby the PFPE coating has higher CAs than the PDMS with most organic working fluids. Patterned wedges of PDMS on a PFPE background provided the highest n-decane condensation rates (up to 3x those on pure PDMS or PTFE coatings), whereby the lower-CA PDMS served as passive transport channels to remove condensate from the surface. Liquid-like PDMS brushes were also shown to promote DWC of ethanol-water mixtures (up to 90% ethanol; 100% ethanol condensation occurred in a filmwise mode) [42].

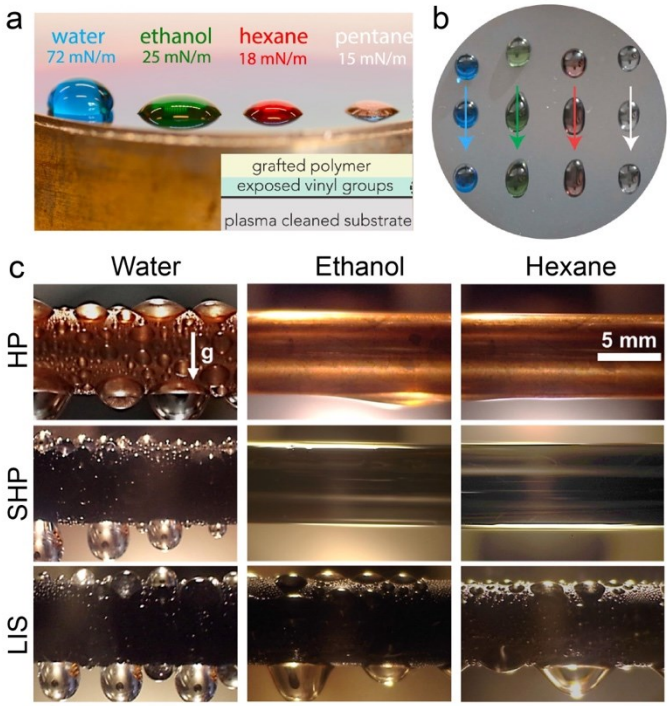

Figure 2 Wettability and condensation of non-aqueous working fluids on different engineered surfaces. Photographs of water, ethanol, hexane and pentane (a) resting and (b) sliding on an initiated chemical vapor deposition (iCVD)-coated metal surface. Reproduced from ref. [39]. (c) Experimental images showing condensation of water, ethanol, and hexane on a smooth hydrophobic Cu tube (HP), silanized nanostructured CuO tube (SHP), and lubricant-infused CuO tube (LIS). The experimental images are from ref. [43].

2.4. Lubricant-infused surfaces for water and non-aqueous dropwise condensation

Another Regime IV-type surface that can promote DWC of both water and non-aqueous working fluids are lubricant-infused surfaces (LISs), often also called slippery liquid-infused porous surfaces (SLIPS). LISs consist of a rough surface infused with a thin (~µm) layer of lubricant, commonly silicone or fluorinated oil. Owing to the liquid nature of the lubricant layer, LISs have many favorable properties, for example, an extremely low CAH even for non-aqueous droplets, allowing for efficient nucleation, growth, and removal of droplets.

While Rykaczewski *et al*. [44] had already qualitatively demonstrated the ability of LISs to promote DWC for working fluids with surface tensions as low at 15 mN/m (*e.g.*, pentane) in 2014, actual heat transfer measurements that quantified the superiority of LISs compared to uncoated surfaces were only recently conducted [43,45–47]. For example, Preston *et al*. [46] found a heat transfer enhancement of ≈450% using toluene as the working fluid (for water, they found a ≈30% enhancement on LISs compared to DWC on a solid hydrophobic surface and ≈400% enhancement compared to FWC on an uncoated surface when carefully removing NCGs from the test chamber). As shown in Fig. 2c, Sett *et al*. [43] demonstrated the superiority of LISs over other engineered surfaces to achieve DWC and reported 200% enhancements in heat transfer using hexane and ethanol. The HTC enhancement for ethanol can be increased to even 8x that of FWC when the condenser is operated with transient pulses, such as shown by Sett *et al*. [48], where ethanol evaporated in-between condensation cycles.

While the benefit of low CAH on LISs is apparent for condensation of low-surface-tension working fluids, LISs have additional advantages over traditional hydrophobic or superhydrophobic surfaces even for water condensation. Firstly, the energy barrier for droplet nucleation is reduced on a liquid or otherwise soft surface as compared to a hard interface [49,50]. Using molecular dynamics simulations, Guo *et al*. [51] confirmed that nucleation of both water and hexane, *i.e*., both cloaked and uncloaked working fluids, are initiated and enhanced at the liquid-air interface. Sharma *et al.* [52] showed experimentally that the nucleation density on silicone-oil infused PDMS increases approximately 10-fold when the substrate shear modulus is decreased from ≈500 kPa to ≈15 kPa. Secondly, oil menisci that naturally form surrounding condensed droplets due to the balance of Laplace pressure and gravity [53] can effectively increase droplet mobility. Sun and Weisensee [54] (using hydrophobic LISs) and later Guo *et al*. [55] (using hydrophilic LISs) showed that once droplets are formed and have grown to a microscopic size through direct vapor accretion or coalescence with their closest neighbors, the overlap of oil menisci can cause rigorous self-propulsion of the microdroplets, as shown in Fig. 3a. This gravity-independent self-propulsion, which is most pronounced for "thick" lubricant films (10s of μm), aids in the frequent clearing of nucleation sites and can significantly enhance nucleation and condensation rates, as demonstrated by Sun *et al.* [56]. For higher degrees of subcooling, when droplets also nucleate on top of the menisci or the (oil-cloaked) droplets [57], Sun and Weisensee [58] recently showed that Marangoni convection within the oil menisci can carry the smallest microdroplets radially away from larger droplets, *i.e.*, carry them towards the colder substrate where they can then grow more efficiently, as shown in Fig. 3b. Using infrared (IR) imaging, Zhu *et al*. [59] observed non-uniform surface temperatures of condensing water droplets, as shown in Fig. 3c, and proposed that larger droplets can also be self-propelled by a thermo-capillary driving force. A very similar propulsion mechanism, where the co-existence of different-sized droplets caused gradients in local temperatures inside small droplets, was also proposed by Teshima *et al*. [60] for low-surface-tension fluids condensing on solid hydrophilic surfaces.

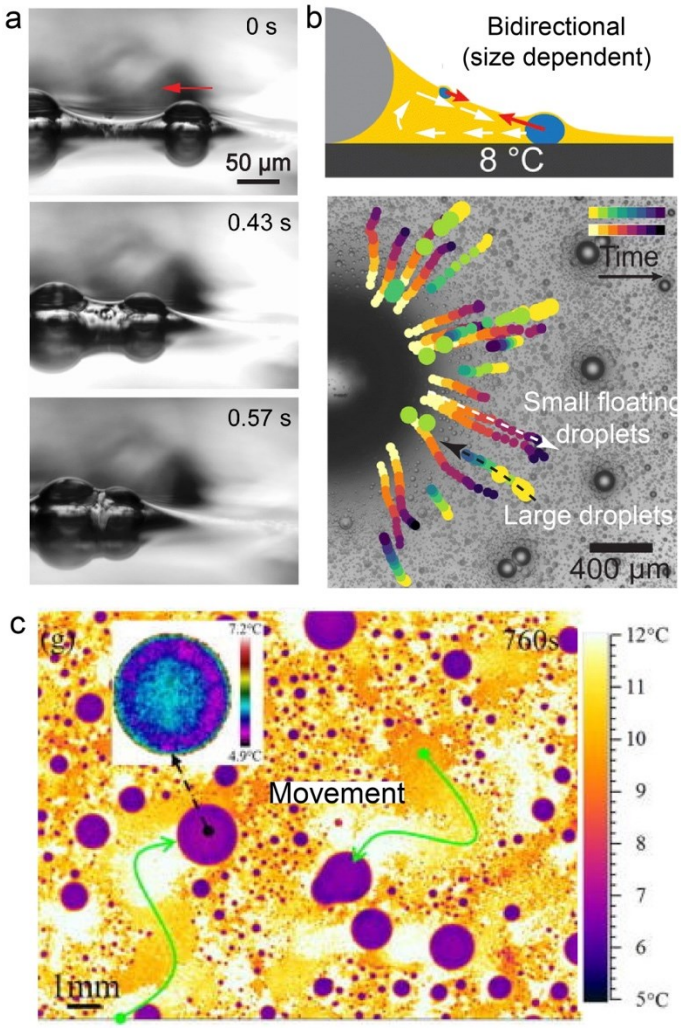

Figure 3: Mobility of different-sized condensed droplets on lubricant-infused surfaces. (a) Microdroplets self-propel long-distances due to an unbalanced capillary force induced by overlapping lubricant menisci. The image is taken from ref. [54] (b) Small floating condensate droplets move down the oil meniscus due to Marangoni convection within the meniscus. The image is adapted from ref. [58] (c) Thermo-capillary movement of millimetric droplets caused by a non-uniform temperature distribution along the triple-phase contact line. Reprinted from [59].

Despite the above-mentioned benefits, the existence of the lubricant also comes with several drawbacks. Firstly, while a thicker oil film promotes droplet self-propulsion, it also poses an enhanced thermal resistance for heat transfer. It can thus be speculated that there exists an optimal lubricant thickness that enables capillary droplet self-propulsion while minimizing the conduction resistance through the film. Secondly, the oil can also pose a fluid dynamic resistance to droplet coalescence. Sun *et al*. [56] showed that at low substrate subcooling, when the nucleation density is relatively low and passive microdroplet propulsion can contribute to faster droplet growth rates, LISs with multiple oil viscosities outperform solid hydrophobic surfaces during moist air water condensation (*e.g.*, dew harvesting). At higher degrees of subcooling, when nucleation densities are high, the relevance of capillary droplet attraction is reduced. Under these conditions, efficient coalescence is key to fast droplet growth. However, on LISs, the oil film must drain from in-between coalescing droplets,

significantly delaying coalescence and growth. Only the LIS with the lowest viscosity studied (Krytox GPL102 with 73 centipose, cP) was on par with the solid hydrophobic surface. These findings highlight the importance of carefully choosing the appropriate coatings for the respective working conditions. Lastly, the lubricant is prone to drainage, as will be discussed in more detail in the following section, which enhances droplet pinning and results in a significant loss of performance within a few hours of operation. A more comprehensive review on advances in condensation on lubricant-infused surfaces can be found in ref. [61]**.**

3. Durability and failure mechanisms of promoter coatings

3.1. Durability concerns of lubricant-infused surfaces

The single-most significant drawback to using LISs in industrial applications is their lack of durability. Although nanostructures (best: nanotubes [62]) can be applied to locally immobilize the lubricant by capillary or van der Waals forces [63], the majority of the lubricant gets removed over time by shear exerted by sliding condensate and – maybe more importantly – as part of the meniscus of shedding droplets [64]. Peppou-Chapman and Neto [65,66] used atomic force microscopy (AFM) to map the degree of lubricant loss on nanostructured surfaces of different surface chemistries and concluded that surface-lubricant-air combinations with a positive spreading coefficient deplete less rapidly (but deplete nonetheless), until an equilibrium lubricant thickness O(10nm) is established. On the other hand, Hoque *et al*. [67] recently showed that the lifetime of the surface can be controlled to a certain extent by choosing appropriate lubricant-working fluid combinations and by increasing the lubricant viscosity. During ethanol condensation on tubes (rather than flat surfaces), the authors demonstrated a lifetime of more than 250 days (as opposed to 45 days for water condensation) when Krytox 16256 (viscosity: μ = 5216 cP) was used. The lifetime was only 10 days for ethanol on Krytox GPL101 with μ = 15 cP. While lubricant viscosity was found to be the more predominant role in increasing the life span of the LIS, the difference in drainage kinetics between water and ethanol condensation was attributed to the existence of a cloaking layer on water, which is absent for ethanol [67]. Contrary to this, Adera *et al*. [68] had concluded in their study on falling droplets from horizontal LIS-tubes that the contribution of the cloaking layer was insignificant to the rate of oil depletion due to its minimal volume (cloaking layer thickness ~20 nm). These contradicting conclusions highlight that a full understanding of the depletion mechanisms during condensation on LISs is still lacking and should be addressed through careful fundamental studies. In our opinion, LISs have a great potential to be used as condensation-enhancing coatings, especially for non-aqueous working fluids, as soon as the challenge of lubricant drainage can be solved.

3.2. Failure mechanisms and new coating strategies for smooth hydrophobic surfaces

Although remarkable dropwise condensation rates have been reported on numerous innovative solid promoter coatings, unfortunately, they are rarely able to maintain dropwise condensation over long periods of time (months, years, or decades), as would be required for their use in industrial applications. Wear-out of thin promoter coatings can lead to surface flooding and the occurrence of FWC [69]. For many years, when new coatings were developed in academia, their performance was

evaluated only for short time periods – usually minutes to hours. Only recently has the "art of lifetime testing", which was more common in the middle of the last century, been re-discovered and expanded upon by a few research groups. Based on heat transfer maximization, the coating thickness should be as thin as possible to decrease its thermal resistances. However, thin coatings ($\lesssim$ 5 μm) usually fail more rapidly [70]. The durability of coatings also depends on how they were applied and at what conditions condensation takes place (*e.g.*, degree of subcooling, moist air *vs*. vapor, or vapor shear flow) [71].

Over the last few years, a small number of studies were dedicated to identifying coating failure modes specific to condensation. Hydrophobic and superhydrophobic coatings can fail when chemical (surface energy) and physical (topographical) inhomogeneities emerge, resulting in a significant increase in CAH and a transition from dropwise to filmwise condensation [72,73]. The failure can be attributed to various factors, including mechanical and chemical damage, the presence of foreign contaminants, or defects within the coating itself. Since most hydrophobic coatings are at the nano or molecular scale, mechanical abrasion can easily remove the coating and expose the underlying hydrophilic substrate. Hence, it is important to exercise extra care during installation and use. Underlying mechanisms of chemical damage are more complicated and vary with the type of working fluid. In a recent study, the chemical durability of flat and patterned crosslinked PDMS surfaces was examined over time under continuous submersion in acidic, basic, and neutral media for various durations [74]. Compared to flat surfaces, patterned surfaces exhibited higher susceptibility to degradation. In the remainder of this discussion, we will primarily focus on the degradation caused by the continuous interplay of growing droplets and vapor on pre-existing defect sites, as this type of failure is more commonly observed during condensation. One of such failure modes is attributed to the formation of blisters due to the accumulation of condensed water between the substrate and the coating [69,75]. Blister delamination was for a long time assumed to be driven by an osmotic pressure difference between liquids across the polymer coating, which could origin either from metal corrosion or solutes/defects at the polymer-substrate interface [76]. Recently, by creating artificial pinholes of approximately 2 μm in diameter on fluorinated hydrophobic films, as illustrated in Fig. 4a, Ma *et al.* [75] showed that film delamination can be caused by the buildup of capillary pressure from water pockets condensing within or on top of the blisters (pinholes). Their results indicated that increasing the interfacial adhesion between the film and the substrate is critical to preventing blistering and enhancing the durability of the coating. Wang *et al*. [69] investigated the degradation of silane self-assembled monolayer (SAM) coatings on silicon substrates during water vapor condensation and hypothesized that the coating degradation initiates at defect sites, *i.e*., uncoated substrate regions, and spreads as condensate breaks down the Si-O-Si bonds between the silane and the substrate, as shown in Fig. 4b. The authors successfully reduced the defect density by suppressing the water/moisture content in the coating fabrication environment and demonstrated that optimized coatings can promote dropwise condensation for hundreds of hours. Another study from the same group [77] investigated degradation of silane SAM coatings on copper surfaces, which are more commonly used in heat exchangers. To obtain pristine and durable SAM coatings on copper requires surface functionalization in pure oxygen plasma before the coating can be applied in an anhydrous environment. Because of the minimal thickness of the SAM coating (< 1 nm),

the copper surface roughness must be minimized. Otherwise, coating defects will occur where condensates can react with uncoated metal patches, reducing cupric oxide (CuO) to cuprous oxide (Cu_2O), which was claimed to result in the possible removal of Si-O-Cu "oxane'' linkage bonds and weaken the overall bonding between silane molecules and the substrate. These novel findings are valuable in developing durable ultrathin coatings on common metal surfaces. In another example, inspired by cell membranes, Ma *et al.* [78] proposed an artificial lipid-like interface that utilizes fluorine–carbon molecular chains to achieve durable nanometric hydrophobic coatings, as shown in Fig. 4c. In contrast to nonpolar chain/fluorinated polymer coatings, the lipid-like coating has strong "wet" adhesion, *i.e.*, strong adhesion even in the presence of water, which can prevent blistering. Superhydrophobic surfaces with such kind of lipid-like interface were able to sustain jumping-droplet-condensation for a continuous one-year steam condensation experiment.

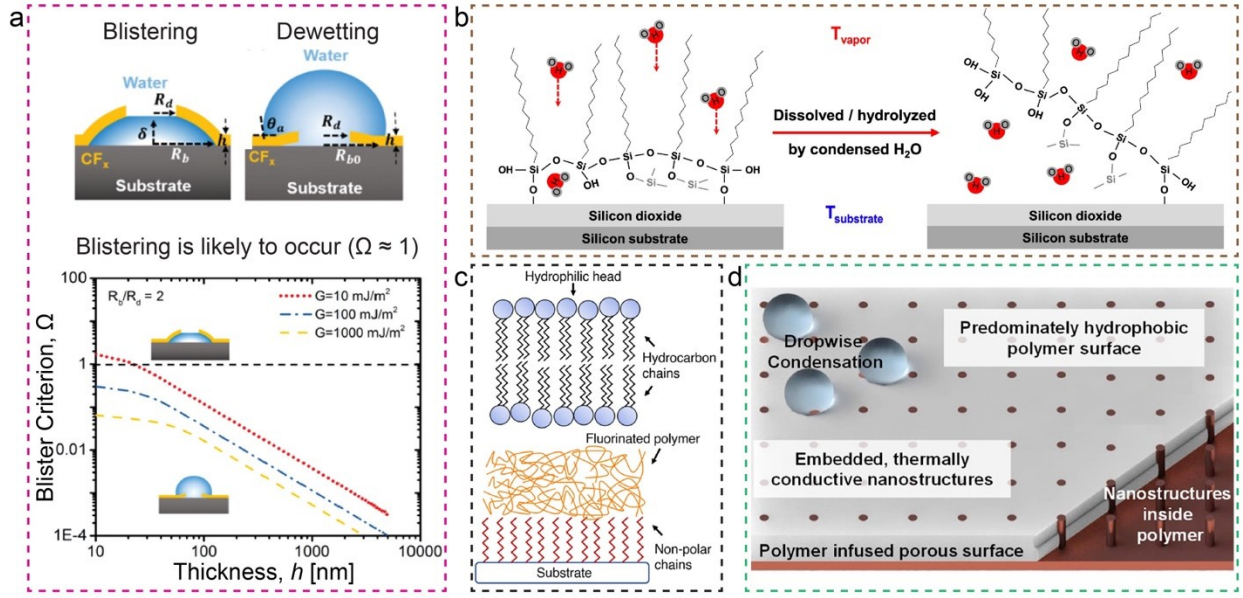

Figure 4: Failure mechanism of hydrophobic coatings and new strategies for improving coating durability. (a) Blistering, or dewetting, on artificial nanoscale pinholes depends on the coating film thickness and the interfacial adhesion. Reproduced from ref. [40]*. (b) Failure mechanism of condensation-mediated degradation of silane self-assembled monolayer (SAM) coatings. The image is from ref.* [69] *(c) An artificial lipid-like interface consists of fluorine–carbon molecular chains, achieving durable nanometric hydrophobic coatings (life span > 1 year). The image is from ref.* [78]*. (d) Polymer infused porous (PIP) surface is made by infusing a thick layer of hydrophobic polymer into a porous microstructured surface, enabling long-lasting DWC (> 200 days). The image is from ref.* [79]*.*

An alternative approach to fabricating smooth, ultra-thin SAM coatings is to create thicker metal-polymer composite coatings. Traditionally, this involved dispersing thermally conductive nanoplatelets or particles into the polymer before applying the coating. However, the thermal resistances at numerous particle-polymer interfaces still limit the overall heat transfer performance [80]. Recently, two research groups concurrently introduced polymer-infused porous (PIP) surfaces [79,81], which are made by infusing a hydrophobic polymer (for example, Teflon AF) into a porous nano/micro-structured surface, as shown in Fig. 4d. Both concepts are based on an earlier work, where sewing needles were poked through a superhydrophobic polymer film to serve as additional nucleation sites and to increase the effective conductivity of the composite coating [82]. Thereby, the coating layer can

be relatively "thick" (10s of µm), which significantly increases the longevity/durability of the coating. Wilke *et al.* [79] demonstrated a more than sevenfold enhancement in condensation heat transfer compared to an uncoated surface, which was sustained for > 200 days without significant degradation. Hatte *et al*. [83] also observed no degradation in performance of similar solid-infused surfaces (SIS) over a 20-day period.

3.3. Wetting transitions on superhydrophobic surfaces

Despite facing a similar issue of blistering and thin film delamination, an even more significant disadvantage of superhydrophobic surfaces is the tendency of water vapor to nucleate within the asperities [84], as shown in Fig. 5a. As droplets grow and coalesce with adjacent droplets, the liquid typically remains trapped within the asperities, eventually flooding the surfaces (*i.e*., transitioning to FWC) [85]. This means that during condensation, superhydrophobic surfaces do not necessarily exhibit the non-wetting Cassie-Baxter state, but rather the wetting Wenzel state. To take advantage of the high condensation performance that non-wetting surfaces can offer, it is of particular interest to transition Wenzel-like (or partial C-B) droplets to a full C-B state. Unfortunately, most of the commonly used stimuli to overcome the energy barrier for this transition, such as external mechanical or magnetic forces, electrowetting, or heating are unsuitable for condensation applications.

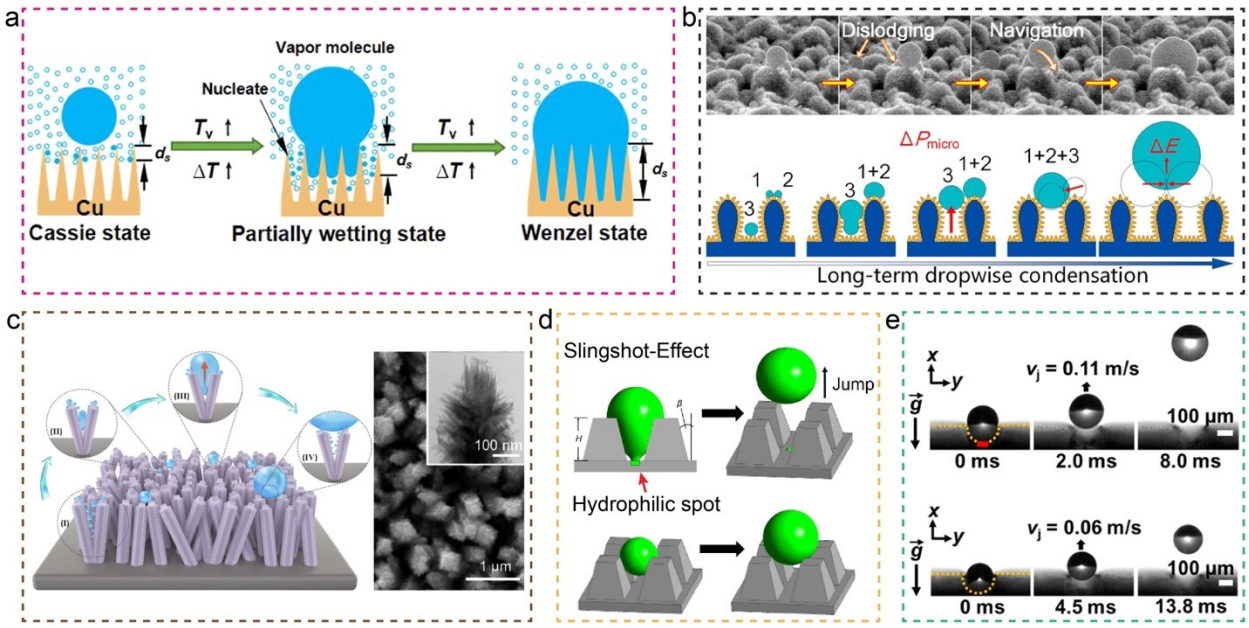

Figure 5: Wetting and de-wetting transitions of condensate droplets on superhydrophobic surfaces. (a) Schematic of the gradual transition of a droplet from the Cassie-Baxter state to a partial wetting state and finally to a Wenzel state due to condensation within structures at increasing degrees of subcooling. The image is from ref. [84]. (b) Condensed droplets spontaneously dislodge from tapered hierarchical structures, inhibiting the wetting transition and sustaining long-term dropwise condensation. The image is from ref. [86]. (c) Complete de-wetting transitions at relatively high subcooling require nano-hierarchical structures. The images are from ref. [87]. (d) Numerical and (e) experimental work on enhanced single-droplet ejection by introducing a hydrophilic spot at the bottom of groove- or pyramid-shaped microstructures. The images are from refs. [88] and [89], respectively.

Recent work has shown promise for using the unbalanced Laplace pressure of tapered micro-/nano-geometries to passively overcome the energy barrier for the de-wetting transition. It is commonly recognized that drops or bubbles confined within tapered geometries can self-propel towards the tapered or wide end of the geometry, depending on whether the meniscus curvature is convex or concave, due to an unbalanced Laplace pressure [90]. As is the case so often, nature has already been using this technique for millennia. For example, cicada wings exhibit spectacular dew repellency and self-cleaning efficiencies [91]. Lecointre, Mouterde, and co-workers conducted systematic experiments on families of conical structures typically found on such cicada wings and showed that condensing droplets, even as small as 1.5 μm in radius, exhibit a highly non-adhesive state on sharp nano-cones across a wide range of texture sizes, apex angles and cone geometries [92,93]. Using Lattice Boltzmann simulations, Zhang *et al*. [94] showed that indeed a spontaneous transition from the (apparent) Wenzel to the C-B state can be induced by changing the adhesion (representative of adding hierarchical nanostructures) at the bottom of conical micro-textures, which was not observed on substrates with straight pillars.

In recent years, many efforts have been devoted to rationally designing scalable structures on metallic surfaces (the most common materials in heat exchangers and many other industrial applications) to promote the de-wetting transition. Sharma *et al*. [95] fabricated truncated micro-cones on copper surfaces using 3D laser micromachining and decorated them with papillae-like nanostructures by chemical etching, onto which a layer of hydrophobic coating was applied. They observed passive droplet ejection from the cavities *via* coalescence of dissimilar-sized droplets. This surface was able to sustain dropwise condensation under vapor shear from saturated steam for eleven days at a low degree of subcooling. Tang *et al*. [86] created micropillars covered with nanograss on copper plates by the process of electrodeposition combined with alkaline oxidation. The upward Laplace pressure induced by the tapered hierarchical micro-nanostructures was able dislodge nucleated microdroplets out of the microgaps and then trigger spontaneous movements on the surfaces, as shown in Fig. 5b. This mechanism can effectively delay flooding and result in a heat transfer coefficient of up to 218 kW/m^2K. It is important to note here that droplets on these hierarchical surfaces are in a Wenzel state from the perspective of the micro-texture, but in a C-B state with respect to the nano-texture, providing sufficiently low adhesion forces to allow for this global wetting transition to occur [96]. Tang *et al.* [97] investigated droplet coalescence during condensation on different nanostructures using large-scale molecular dynamics simulations and found that a low height and large spacing between nanostructures, as often caused by mechanical damage, can severely degrade the ability of a surface to promote the Wenzel-to-Cassie wetting transition.

At higher degrees of subcooling, preventing hierarchical superhydrophobic surfaces from flooding poses an even bigger challenge. According to the classical nucleation theory, at a surface subcooling of 4 K the critical nucleation size is approximately 5 nm [98] – small enough to nucleate even with in the nano-textures and negating the ejection-effect from the micro-textures. Therefore, the Laplace pressure driven mechanism must be scaled down to the nanoscale. Figure 5c shows a nano-hierarchical structured surface that was developed by Song *et al*. [87] by growing branched TiO_2

nanorod arrays, which is also capable of pushing nanodroplets out of the nanostructures. By introducing a hydrophilic spot at the bottom of groove- or pyramid-shaped microstructures, unprecedentedly fast single-droplet ejection has been demonstrated both experimentally and numerically [88,89], as shown in Figs. 5d and 5e. The hydrophilic spots – once optimized for their size – serve two purposes. First, they increase the deformational stretching of the confined nanodroplets, ultimately leading to a higher conversion potential of surface energy to kinetic energy. Second, they serve as local nucleation sites, promoting a higher nucleation rate. Laplace-pressure-driven droplet ejection can potentially reduce the droplet departure volume and thereby increase the frequency of condensation cycles and heat transfer rates. In the following section, we will present other recent novel designs to enhance droplet removal.

4. Strategies for condensate removal

Continuously and effectively removing condensates from the surface is critical to sustaining dropwise condensation. The most common and universal way is gravitational shedding, which becomes relevant for droplet sizes O(1mm). Droplets sliding down the surface can effectively remove other droplets along the sweeping path, exposing a fresh surface for re-nucleation. However, this method is not very efficient and contingent on the surface orientation and surface properties. To actively remove condensate droplets below the gravitational size limit, various approaches have been proposed, which can be generally categorized into two types: innovate surface designs to passively shed droplets and external stimuli to actively remove droplets.

4.1. Passive surface designs

Generally, passive surface designs are based on the rational design of anisotropic structures or surface wettabilities. For example, micrometric or millimetric grooves can efficiently transport the condensate laterally and improve the overall heat transfer rate [99–102]. Surface structures also improve the efficiency of out-of-plane droplet removal, as recently shown by Ma *et al.* [103], who created superhydrophobic thin-walled micro-lattice structures, as shown in Fig. 6a. Such a surface design imposes physical restrictions on the size of jumping droplets, thereby leading to a 100% probability of jumping above a given droplet size, as determined by the dimensions of the lattice structures. This structure resulted in a 34% enhancement of the HTC compared to a planar superhydrophobic surface at a subcooling of 1 K in pure steam condensation.

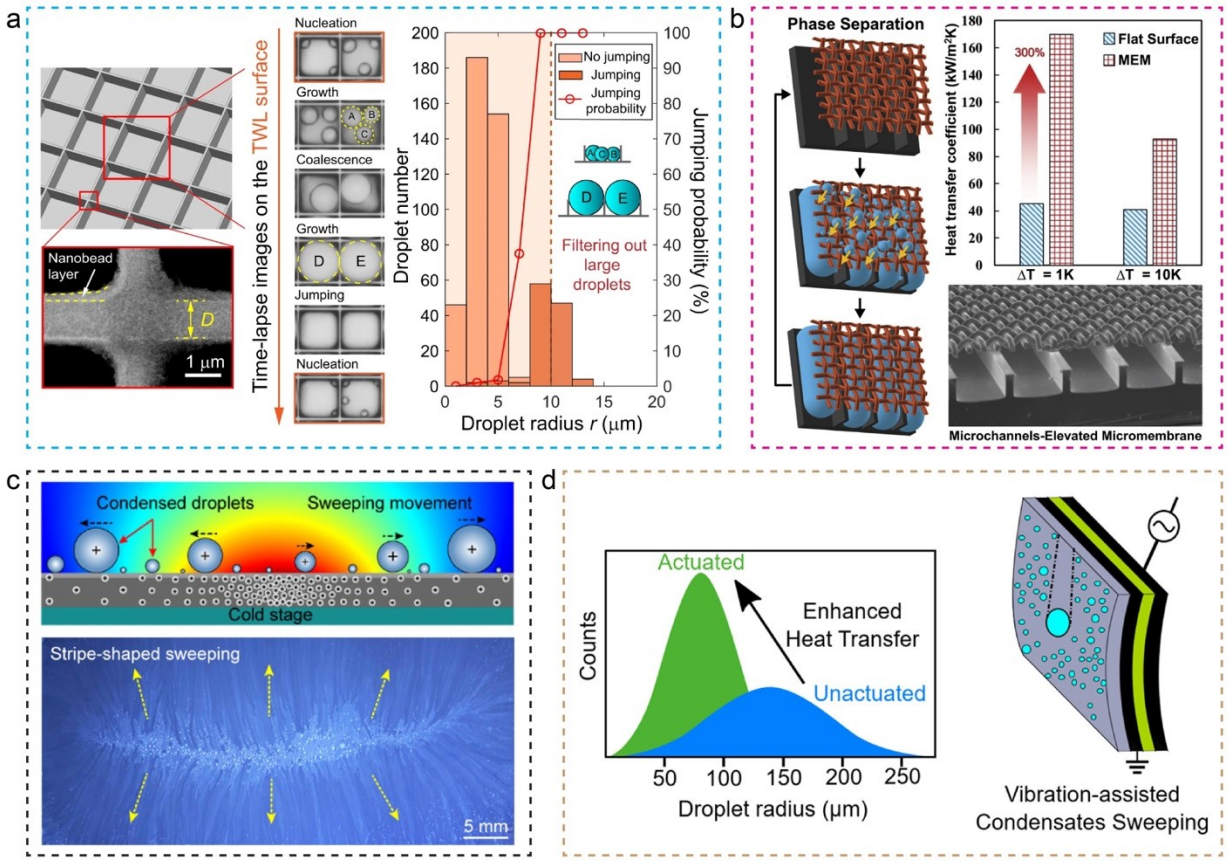

Figure 6: Examples of passive and active droplet removal strategies. (a) Spontaneous removal of condensate droplets with controlled sizes on superhydrophobic thin-walled micro-lattice structures. Reprinted from ref. [103]. (b) A microchannels-elevated micromembrane (MEM) composite surface can increase the heat transfer coefficient up to 300%, whereby the micromembrane separates vapor and liquid flow and slippery microchannels remove the condensate. Reproduced from ref. [104]. (c) Directional transport of condensed droplets on a superhydrophobic with a strip-shaped positive charge density gradient (CDG). Reprinted from ref. [105]. (d) A higher fraction of small droplets (< 100 μm) increases the heat transfer on vibrating lubricant-infused nano-porous surfaces due to vibration-assisted droplet sweepings. Reproduced from ref. [106].

Except for SLIC surfaces, surfaces with uniform wettability can be either optimized for enhanced nucleation or for enhanced droplet mobility. For more than a decade, wettability-patterning surfaces has thus been used to synergistically take advantage of hydrophilicity for nucleation and hydrophobicity for droplet transport [107]. Recent work has focused on optimizing the geometry of these bi-philic surfaces, characterizing droplet behavior and heat transfer rates, and developing scalable fabrication methods [108–110]. For example, Boylan *et al.* [111] designed an ultra-smooth biphilic surface consisting of PEGylated (hydrophilic) and siloxane polymers (hydrophobic) quasi-liquid surfaces (QLS). Owing to their extremely low CAH, heat transfer rates on these biphilic QLS more than doubled compared to commonly used hydrophobic silane surfaces, for both atmospheric water harvesting and pure steam condensation. As already discussed in section 3.3, wettability-patterning can also increase the efficiency of jumping droplet condensation. Another such example is given in the work of Zhu *et al*. [112], who seeded hydrophilic sites on top of a superhydrophobic substrate, which maximized the

droplet jumping height and led to 61% higher water harvesting rates compared to a plain superhydrophobic surface.

Of course, the two concepts of structural and wettability patterning can also be combined [113–115]. These integrated surfaces can achieve remarkable enhancement in heat transfer rates and sustain DWC even at high degrees of subcooling. Shan *et al.* [104] designed a novel microchannel-elevated micromembrane (MEM) surface, as shown in Fig. 6b, where the hydrophobic micromembrane can separate the vapor and liquid and then condensed water is transported through the slippery microchannels. Sustained dropwise condensation was reported at a subcooling of 10 K, featuring a heat flux of 1000 kW/m^2. In an effort to increase the applicability and durability of hierarchical surface designs, Winter and McCarthy [116] micromachined amphiphilic aluminum channels that were coated on the top with a thick (and hence durable) layer of hydrophobic rubber. The water nucleated within the hydrophilic channels, but spontaneously dewetted the channels upon reaching a critical size. Once droplets emerged from the channels, they were removed from the hydrophobic fins *via* gravitational shedding, promoting new condensate growth within the channel.

Another novel passive condensate removal technique takes advantage of contact electrification of droplets, whereby charges separate at the solid-liquid interface and positively charge the droplet upon droplet sliding [117,118] or jumping [119]. By applying a charge density gradient (CDG) of positive ions on a superhydrophobic surface using a corona discharge emitter, Zhang *et al.* [105] reported fast sweeping of small droplets (size: 20-30 μm), as shown in Fig. 6c, which contributes to a high droplet removal rate, a high number density of small droplets, and low droplet surface coverage.

4.2. External stimuli

In addition to employing passive approaches to facilitate coalescence and shedding of condensates, adopting external stimuli has also been widely studied. Again, taking advantage of droplet charging during condensation, an external electric field can be applied, which can prevent jumping droplets from returning to the surfaces [120]. Electric fields also influence water nucleation, as shown by Wang *et al*. [121,122] using molecular dynamics simulations. The size of the critical nucleus and the nucleation time increase with the frequency of the AC electric field. The authors also showed that the nucleation time first decreases and then increases with the intensity of the electric field when applied parallel to the surface. By elongating vapor clusters, moderate electric fields also increase the probability of cluster coalescence. Hence, an optimal voltage exists to achieve the best condensation efficiency. Similarly, electrowetting on dielectric (EWOD) influences the mobility of larger droplets by changing their contact angle and coalescence dynamics [123,124]. A recent study from Wikramanayake *et al*. [125] showed that AC-electrowetting can decrease the time-averaged droplet surface coverage to as low as 2%, depending primarily on the magnitude of the electric field (whereby the AC frequency dictated the time constant for droplet removal). Consequently, the condensed mass flux was more than two orders of magnitude higher than without an electric field or a continuous electric field.

While electrowetting can effectively enhance coalescence and condensation rates, its cumbersome microfabrication makes it unsuitable for many applications. Recently, Oh *et al*. [106] thus

presented an alternative that applies bulk vibrational actuation to a slippery liquid-infused nanoporous surface (SLIPS), as shown in Fig. 6d, whereby the radius and speed of the departing droplets were decreased and increased, respectively, by 39% and 860%. These enhanced droplet dynamics led to a lower surface coverage and a higher fraction of small droplets (< 100 μm), effectively enhancing the overall heat transfer.

The above-mentioned methods are only a small selection of current and past strategies to enhance droplet removal with the goal of enhancing condensation rates and/or preventing surface flooding. A central disadvantage to most active removal strategies are the sophisticated sample design and continuous energy consumption. However, for certain applications, for example those that cannot rely on gravity to shed the condensate, such as in mobile devices or micro-gravity environments, active strategies can ensure a reliable condensation performance. Nonetheless, researchers working in these fields should account for high energy efficiency and scalability when proposing new methods.

5. Conclusion and outlook

The last few years have brought significant advances in the theoretical understanding and the practical implementation of dropwise condensation for water and non-aqueous working fluids. Guided by the appreciation that droplet mobility, not surface wettability *per se*, dictates the mode of condensation, researchers have developed ultra-smooth coatings, such as liquid-like solid surfaces or lubricant-infused surfaces that exhibit extremely low CAH and DWC with most working fluids. LISs have the added benefit of promoting rigorous microdroplet self-propulsion, which can enhance (water) condensation rates at low and intermediate subcooling temperatures (at high subcooling, however, the coalescence delay due to oil drainage can impede efficient heat transfer). Based on theoretical considerations, the critical heat flux (CHF) for the transition from dropwise to filmwise condensation is of the order of 10 MW/m² at a subcooling of 20 K (heat transfer coefficient: h ~ 10^2-10^3 kW/m²K) [126,28]. This value is considerably higher than the typical operating range of most practical condensers, and also significantly higher than any experimentally achieved heat transfer rates to date, which are on the order of hundreds of kW/m² to ~ 2 MW/m² and up to 300 kW/m²K at low subcoolings (1-8K) [71,104,111,127–129]. Despite the high deviation from ideal heat transfer rates, these recent advances in pushing condensation rates are remarkable when considering heat transfer coefficients of <20 kW/m²K for traditional filmwise condensation. Unfortunately, however, most of these surfaces suffer from degradation, such as blistering and delamination (solid coatings) or lubricant loss (LISs). Recent work has explored some of the common failure mechanisms and used these insights to develop new fabrication techniques, for example coating deposition in anhydrous environments. Despite these advancements towards sustainably enhancing the heat transfer during condensation of water and organic working fluids, substantial research efforts are still needed to make these solutions viable for industrial settings. In the following, we briefly give an overview over five exemplary topic areas, which we believe – once solved – will have a significant impact on condensation heat transfer applications.

In-situ coating degradation – In section 3.2 we introduced some of the recent advances towards better understanding the failure mechanisms during DWC, yet much remains to be done in this regard.

When developing new condensation heat transfer coatings, it is thus crucial to focus not only on achieving short-term high performance gains, but also on conducting thorough durability analyses. To make results more comparable, the community should develop a set of standards and testing procedures for such lifetime characterizations. Secondly, future research should involve multi-disciplinary teams (including materials scientists and/or polymer chemists) that study the evolution of defects during condensation *in-situ* (*i.e.*, *in-operando*) for different working conditions (*e.g.*, high subcooling, vapor shear flow, pure steam *vs*. moist air *vs*. organic working fluid). Rather than relying on "trial-and-error" coating design approaches and degradation "anecdotes", rigorous physics- or chemistry-based models should be established, based on which new coating chemistries can then be identified and developed.

Pure vapor vs. moist air – As briefly alluded to in the introduction (section 1), it is extremely important to differentiate between condensation of pure vapor *vs*. condensation from moist air, since the thermodynamics of these two conditions are vastly different. Not only does moist-air condensation move the dominating heat transfer resistance to the gas-diffusion layer, rather than the condensate, it also enhances the deposition of volatile organic compounds (VOCs) and airborne salts on the surface, which on the one hand can temporarily increase the nucleation density on the surface, but on the other hand can also lead to surface fouling and heat transfer degradation [130–132]. Due to these vastly varying conditions (including coating failure, as discussed above), we suggest that researchers be more deliberate in choosing and clearly articulating the condition for which their surfaces and coatings are designed for. There is no (need for) "one size fits all", but very often, researchers (including ourselves) conduct experiments in moist air for its simplicity in setup, while aiming at pure vapor environments for applications. This disparity is likely one of the reasons that tech-transfer from the academic laboratory to industry has been relatively slow in this field. To facilitate comparisons between different surfaces (and real-world condensers), care must be taken to fully de-gas the working fluid for pure vapor experiments, since already miniscule amounts of NCGs can significantly influence the measured heat transfer rates [133]. The NCGs present in working fluids can be effectively removed through vigorous boiling. Generally, there are two methods to minimize the presence of NCGs in the apparatus (including the condensation chamber and tubes). The first approach involves vacuuming the system down to < 1 Pa prior to injecting pure vapor, which is the most commonly adopted approach [39,40,43,79]. To build such a custom-designed system, however, requires expertise in vacuum technology and demands a substantial amount of time and financial resources. On the other hand, the second method is relatively easier to implement and relies on expelling the air by continuously supplying superheated steam at a positive pressure (few kPa above atmosphere pressure) for multiple hours before taking heat transfer measurements [32,128]. The second method has some limitations, wherein the amount of NCGs in the chamber is unknown and only estimated *via* validation experiments, and the vapor temperature needs to be consistently over 100°C. Furthermore, the condensation mode closely resembles forced convection condensation due to a certain steam velocity. Generally, we would encourage research groups to provide more details on their apparatus and testing procedures, for example as part of a

supplementary information (an excellent demonstration of such documentation can be found in these references [43,134]).

Non-aqueous working fluids – While academic research has placed a strong emphasis on water condensation on external surfaces (partly because of its ease in experimentation), increasing the condensation efficiency of non-aqueous working fluids will become increasingly important. One avenue the phase change research community can take to address climate change is the development of higher-efficiency low-grade heat power generation cycles and air conditioning and refrigeration systems (including heat pumps), to all of which the condensation of an organic working fluid (*e.g.*, refrigerant) is central. In section 2.3 we briefly discussed the development of ultra-smooth polymer coatings and the use of LISs to achieve DWC for these fluids. More research needs to be conducted to better understand the durability of these coatings for non-aqueous condensation. An alternative approach, which does not require defect-free low-surface-energy coatings, could be the resurrection of Marangoni condensation of dilute binary mixtures. During Marangoni condensation, also called pseudo-dropwise condensation, the condensate first develops as a thin film and then breaks up into droplets due to fluid instabilities, which is independent of surface wettability. While most commonly observed for water-alcohol mixtures [9], early work from the 1960s demonstrated Marangoni condensation for low-surface tension fluids, such as methanol + n-pentane or n-hexane, benzene + n-pentane (n-hexane), and methylene chloride (= dichloromethane) + n-pentane [135,136]. It stands to reason that modern-day refrigerants could also condense in a pseudo-dropwise mode, which could potentially enable an up to 10-fold wettability-independent enhancement in condensation rates.

Nucleation – Any condensation process starts with and is heavily influenced by nucleation, yet we know so little about. The classical nucleation theory (CNT) gives a dependence on substrate wettability and subcooling, but it is too inaccurate to predict real nucleation rates or densities. At common vapor and substrate temperatures, the critical nucleation size is O(1-10 nm) – too small to visualize using visible light. Many experimentalists (including ourselves) thus assume that the number of smallest visibly detectable droplets (≈ 1 μm in diameter) approximately corresponds to the number of nucleated droplets [22,56,130]. The validity of this assumption is, however, far from certain. Zhang *et al*. [137] developed a technique based on phase-enhanced environmental scanning electron microscopy (p-ESEM) to study nucleation dynamics. However, even this electron-based technique has a limited spatial resolution of ≈ 0.5 μm – very comparable to high-quality optical microscopy setups and still orders of magnitude larger than the smallest nuclei. Transmission electron microscopy (TEM) can achieve finer resolutions, but is limited in its range of working conditions and requires very tedious sample preparation [138]. Due to the lack of reliable visualization techniques, reported nucleation densities hence vary over many orders of magnitude. Yet many models (both computational and theoretical) rely on an accurate knowledge of nucleation densities and rates. Currently, nucleation in computational models that have been developed to predict heat transfer rates during condensation is initiated using a seemingly random ("best guess") nucleation density. New imaging techniques are hence necessary to better characterize nucleation densities and kinetics on surfaces with varying wettabilities and under a wide range of operating temperatures. An example could be scattering-based techniques, which have

long been used in the aerosol community to statistically determine the size distribution of very small droplets [139]. Additionally, with the advancements in molecular dynamics simulations using water as the working fluid, numerical approaches should be developed that bridge the gap between nanoscopic and microscopic simulation domains, which would enable an easier comparison and validation with experimental data.

Models for dynamic condensation processes – Condensation is an extremely dynamic process, especially when occurring on lubricant-infused and other soft surfaces, as discussed in section 2.4. However, virtually every researcher wanting to predict (or confirm) heat transfer rates during DWC uses a theoretical model made popular by Rose, Le Fèvre, and Glicksman [133], in which the per-droplet heat flux (taking into account conduction and interfacial resistances) is integrated over the average size distribution of droplets on the surface. This size distribution of large droplets (>1-10 μm) is typically determined by taking a few sequential still photos of the surface during steady-state condensation and averaging the observed numbers of droplets. Then, the size distribution of small droplets (with a radius smaller than the coalescence radius) is obtained *via* the population balance theory [140]. Two possible concerns arise with this approach. First, the spatial resolution of the imaging setup that many researchers apply is not fine enough to detect droplets smaller than O(10 μm), despite the significant importance of these small droplets towards condensation heat transfer rates (more than half of the heat is transferred by droplets smaller than 10 μm [141]). Second, this approach is unable to reflect any dynamic effects, such as capillary self-propulsion, Marangoni-induced droplet transport, or other droplet propulsion and removal processes. For example, Weisensee *et al*. [141] found that for water condensation on LISs, the time-averaged droplet size distribution is independent of the lubricant viscosity and its cloaking tendency. On the other hand, in a subsequent study, Sun *et al*. [56] found that the lubricant viscosity has a very strong influence on both the nucleation rate density and the water collection rate. Since we used very similar experimental conditions for both studies, one can conclude that the time-averaged droplet size distribution does not accurately reflect the actual condensation heat transfer process. We thus propose that new theoretical models should be developed alongside new surfaces and droplet removal strategies, which consider dynamic (or transient) droplet processes. Guo *et al*. [142] recently developed a dynamic model for DWC that is based on Rose's model, but additionally introduces a semi-empirical droplet disappearance frequency to account for droplet capillary self-propulsion and enhanced coalescence rates. We believe this is an important first step towards dynamic heat transfer modeling, with future models being based on rigorous theoretical developments. For jumping-droplet condensation, Zhang *et al*. [140] found that the instantaneous droplet population change is mainly due to the coalescence between droplets and subsequent jumping and developed governing equations for the overall size distribution incorporating properties of superhydrophobic surfaces. The prediction from the proposed model showed good agreement with previous experiments.

A promising alternative approach to modeling dynamic condensation processes could lie in the use of machine learning (ML). Researchers have recently implemented a vision-based deep learning framework for studying dropwise condensation, which consists of droplet detection, tracking and data process modules [143–145]. By tracking droplet growth or counting falling droplets, multi-level physical

descriptors such as droplet growth rate, transient heat flux, and droplet distributions can be extracted with an uncertainty of less than 10% during condensation on hydrophobic surfaces at low heat fluxes [144]. However, the current model still requires further enhancement to accurately characterize jumping-droplet condensation or condensation on LISs due to unique droplet mobility and departure mechanisms. Overall, we believe that ML can be a potent alterative in revisiting the existing semi-empirical DWC theory and offers a cost-effective method for local heat transfer measurements without the need for temperature sensors [5,146]. Apart from algorithmic advancements, however, the performance of ML (such as accuracy and generalizability) heavily relies on extensive training data and encourages the open sharing of data. Over the past decades, a wealth of experimental data has been accumulated in the field of condensation. Establishing an open-source database, to which all experimentalists can contribute, would significantly bolster the application of ML in condensation processes and help deepen our comprehension of the underlying physics.

Acknowledgement

J.S. and P.B.W. would like to acknowledge support from the U.S. National Science Foundation through awards No. 1856722 and No. 2147483.

References

[1] Beard KV, Ochs HT. Warm-Rain Initiation: An Overview of Microphysical Mechanisms. J Appl Meteor 1993;32:608–25. https://doi.org/10.1175/1520-0450(1993)032<0608:WRIAOO>2.0.CO;2.
[2] Tu R, Hwang Y. Reviews of atmospheric water harvesting technologies. Energy 2020;201:117630. https://doi.org/10.1016/j.energy.2020.117630.
[3] Dirker J, Juggurnath D, Kaya A, Osowade EA, Simpson M, Lecompte S, et al. Thermal Energy Processes in Direct Steam Generation Solar Systems: Boiling, Condensation and Energy Storage – A Review. Front Energy Res 2019;6:147. https://doi.org/10.3389/fenrg.2018.00147.
[4] Pattanayak L, Padhi BN, Kodamasingh B. Thermal performance assessment of steam surface condenser. Case Studies in Thermal Engineering 2019;14:100484. https://doi.org/10.1016/j.csite.2019.100484.
[5] Upot NV, Fazle Rabbi K, Khodakarami S, Ho JY, Kohler Mendizabal J, Miljkovic N. Advances in micro and nanoengineered surfaces for enhancing boiling and condensation heat transfer: a review. Nanoscale Adv 2023:10.1039.D2NA00669C. https://doi.org/10.1039/D2NA00669C.
[6] Wang Z-J, Wang S-Y, Wang D-Q, Yang Y-R, Wang X-D, Lee D-J. Water vapor condensation on substrates with nanoscale hydrophilic spots: A molecular dynamics study. International Journal of Heat and Mass Transfer 2023;205:123929. https://doi.org/10.1016/j.ijheatmasstransfer.2023.123929.
[7] Sokuler M, Auernhammer GK, Roth M, Liu C, Bonacurrso E, Butt H-J. The Softer the Better: Fast Condensation on Soft Surfaces. Langmuir 2010;26:1544–7. https://doi.org/10.1021/la903996j.
[8] Wen R, Zhou X, Peng B, Lan Z, Yang R, Ma X. Falling-droplet-enhanced filmwise condensation in the presence of non-condensable gas. International Journal of Heat and Mass Transfer 2019;140:173–86. https://doi.org/10.1016/j.ijheatmasstransfer.2019.05.110.

[9] Jivani S, Liu JH, Pu JH, Wang HS. Marangoni condensation of steam-ethanol mixtures on a horizontal smooth tube. Experimental Thermal and Fluid Science 2021;128:110434. https://doi.org/10.1016/j.expthermflusci.2021.110434.
[10] Riley GA, Mendez CE, Egbo M, Hwang G, Derby MM. Visualizing and disrupting liquid films for filmwise flow condensation in horizontal minichannels. Front Therm Eng 2022;2:953051. https://doi.org/10.3389/fther.2022.953051.
[11] Ho JY, Leong KC. A critical review of filmwise natural and forced convection condensation on enhanced surfaces. Applied Thermal Engineering 2021;186:116437. https://doi.org/10.1016/j.applthermaleng.2020.116437.
[12] Thomas TM, Sinha Mahapatra P, Ganguly R, Tiwari MK. Preferred Mode of Atmospheric Water Vapor Condensation on Nanoengineered Surfaces: Dropwise or Filmwise? Langmuir 2023:acs.langmuir.3c00022. https://doi.org/10.1021/acs.langmuir.3c00022.
[13] Schmidt E, Schurig W, Sellschopp W. Versuche über die Kondensation von Wasserdampf in Film- und Tropfenform. Technische Mechanik und Thermodynamik 1930;1:53–63. https://doi.org/10.1007/BF02641051.
[14] El Fil B, Kini G, Garimella S. A review of dropwise condensation: Theory, modeling, experiments, and applications. International Journal of Heat and Mass Transfer 2020;160:120172. https://doi.org/10.1016/j.ijheatmasstransfer.2020.120172.
[15] Goswami A, Pillai SC, McGranaghan G. Surface modifications to enhance dropwise condensation. Surfaces and Interfaces 2021;25:101143. https://doi.org/10.1016/j.surfin.2021.101143.
[16] Ho JY, Rabbi KF, Khodakarami S, Ma J, Boyina KS, Miljkovic N. Opportunities in Nano-Engineered Surface Designs for Enhanced Condensation Heat and Mass Transfer. Journal of Heat Transfer 2022;144:050801. https://doi.org/10.1115/1.4053454.
[17] Miljkovic N, Enright R, Nam Y, Lopez K, Dou N, Sack J, et al. Jumping-Droplet-Enhanced Condensation on Scalable Superhydrophobic Nanostructured Surfaces. Nano Lett 2013;13:179–87. https://doi.org/10.1021/nl303835d.
[18] Ahlers M, Buck-Emden A, Bart H-J. Is dropwise condensation feasible? A review on surface modifications for continuous dropwise condensation and a profitability analysis. Journal of Advanced Research 2019;16:1–13. https://doi.org/10.1016/j.jare.2018.11.004.
[19] Preston DJ, Wang EN. Jumping Droplets Push the Boundaries of Condensation Heat Transfer. Joule 2018;2:205–7. https://doi.org/10.1016/j.joule.2018.01.011.
[20] Tuteja A, Choi W, Ma M, Mabry JM, Mazzella SA, Rutledge GC, et al. Designing Superoleophobic Surfaces. Science 2007;318:1618–22. https://doi.org/10.1126/science.1148326.
[21] Quéré D. Wetting and Roughness. Annual Review of Materials Research 2008;38:71–99. https://doi.org/10.1146/annurev.matsci.38.060407.132434.
[22] Katselas A, Parin R, Neto C. Quantification of Nucleation Site Density as a Function of Surface Wettability on Smooth Surfaces. Advanced Materials Interfaces 2022;9:2200246. https://doi.org/10.1002/admi.202200246.
[23] Wang S-Y, Wang Z-J, Wang D-Q, Yang Y-R, Zheng S-F, Gao S-R, et al. Nucleation of water vapor on nanodimpled surfaces: Effects of curvature radius and surface wettability. Applied Thermal Engineering 2023;219:119437. https://doi.org/10.1016/j.applthermaleng.2022.119437.
[24] Misra S, Teshima H, Takahashi K, Mitra SK. Reflected Laser Interferometry: A Versatile Tool to Probe Condensation of Low-Surface-Tension Droplets. Langmuir 2021;37:8073–82. https://doi.org/10.1021/acs.langmuir.1c00145.
[25] Neumann AW, Abdelmessih AH, Hameed A. The role of contact angles and contact angle hysteresis in dropwise condensation heat transfer. International Journal of Heat and Mass Transfer 1978;21:947–53. https://doi.org/10.1016/0017-9310(78)90186-2.

[26] Chu F, Wu X, Zhu Y, Yuan Z. Relationship between condensed droplet coalescence and surface wettability. International Journal of Heat and Mass Transfer 2017;111:836–41. https://doi.org/10.1016/j.ijheatmasstransfer.2017.04.052.
[27] Anand S, Paxson AT, Dhiman R, Smith JD, Varanasi KK. Enhanced Condensation on Lubricant-Impregnated Nanotextured Surfaces. ACS Nano 2012;6:10122–9. https://doi.org/10.1021/nn303867y.
[28] Cha H, Vahabi H, Wu A, Chavan S, Kim M-K, Sett S, et al. Dropwise condensation on solid hydrophilic surfaces. Sci Adv 2020;6:eaax0746. https://doi.org/10.1126/sciadv.aax0746.
[29] Nakamura S, Archer RJ, Dunderdale GJ, Hozumi A. Perfluorinated compounds are not necessary: pegylated organosilanes can endow good water sliding/removal properties. Journal of Hazardous Materials 2020;398:122625. https://doi.org/10.1016/j.jhazmat.2020.122625.
[30] Vahabi H, Vallabhuneni S, Hedayati M, Wang W, Krapf D, Kipper MJ, et al. Designing non-textured, all-solid, slippery hydrophilic surfaces. Matter 2022;5:4502–12. https://doi.org/10.1016/j.matt.2022.09.024.
[31] Miljkovic N, Enright R, Wang EN. Effect of Droplet Morphology on Growth Dynamics and Heat Transfer during Condensation on Superhydrophobic Nanostructured Surfaces. ACS Nano 2012;6:1776–85. https://doi.org/10.1021/nn205052a.
[32] Monga D, Guo Z, Shan L, Taba SA, Sarma J, Dai X. Quasi-Liquid Surfaces for Sustainable High-Performance Steam Condensation. ACS Appl Mater Interfaces 2022;14:13932–41. https://doi.org/10.1021/acsami.2c00401.
[33] Paxson AT, Varanasi KK. Self-similarity of contact line depinning from textured surfaces. Nat Commun 2013;4:1492. https://doi.org/10.1038/ncomms2482.
[34] Qu X, Boreyko JB, Liu F, Agapov RL, Lavrik NV, Retterer ST, et al. Self-propelled sweeping removal of dropwise condensate. Appl Phys Lett 2015;106:221601. https://doi.org/10.1063/1.4921923.
[35] Boreyko JB, Chen C-H. Self-Propelled Dropwise Condensate on Superhydrophobic Surfaces. Phys Rev Lett 2009;103:184501. https://doi.org/10.1103/PhysRevLett.103.184501.
[36] Preston DJ, Wang EN. Jumping Droplets Push the Boundaries of Condensation Heat Transfer. Joule 2018;2:205–7. https://doi.org/10.1016/j.joule.2018.01.011.
[37] Mulroe MD, Srijanto BR, Ahmadi SF, Collier CP, Boreyko JB. Tuning Superhydrophobic Nanostructures To Enhance Jumping-Droplet Condensation. ACS Nano 2017;11:8499–510. https://doi.org/10.1021/acsnano.7b04481.
[38] Yan X, Zhang L, Sett S, Feng L, Zhao C, Huang Z, et al. Droplet Jumping: Effects of Droplet Size, Surface Structure, Pinning, and Liquid Properties. ACS Nano 2019:acsnano.8b06677. https://doi.org/10.1021/acsnano.8b06677.
[39] Khalil K, Soto D, Farnham T, Paxson A, Katmis AU, Gleason K, et al. Grafted Nanofilms Promote Dropwise Condensation of Low-Surface-Tension Fluids for High-Performance Heat Exchangers. Joule 2019;3:1377–88. https://doi.org/10.1016/j.joule.2019.04.009.
[40] Fazle Rabbi K, Ho JY, Yan X, Ma J, Hoque MJ, Sett S, et al. Polydimethylsiloxane-Silane Synergy enables Dropwise Condensation of Low Surface Tension Liquids. Adv Funct Materials 2022;32:2112837. https://doi.org/10.1002/adfm.202112837.
[41] Soltani M, Golovin K. Lossless, Passive Transportation of Low Surface Tension Liquids Induced by Patterned Omniphobic Liquidlike Polymer Brushes. Adv Funct Materials 2022;32:2107465. https://doi.org/10.1002/adfm.202107465.
[42] Li S, Diaz D, Kappl M, Butt H, Liu J, Hou Y. Enhanced condensation heat transfer by water/ethanol binary liquids on polydimethylsiloxane brushes. Droplet 2022;1:214–22. https://doi.org/10.1002/dro2.31.

[43] Sett S, Sokalski P, Boyina K, Li L, Rabbi KF, Auby H, et al. Stable Dropwise Condensation of Ethanol and Hexane on Rationally Designed Ultrascalable Nanostructured Lubricant-Infused Surfaces. Nano Lett 2019;19:5287–96. https://doi.org/10.1021/acs.nanolett.9b01754.
[44] Rykaczewski K, Paxson AT, Staymates M, Walker ML, Sun X, Anand S, et al. Dropwise Condensation of Low Surface Tension Fluids on Omniphobic Surfaces. Sci Rep 2014;4. https://doi.org/10.1038/srep04158.
[45] Seo D, Shim J, Shin DH, Nam Y, Lee J. Dropwise condensation of acetone and ethanol for a high-performance lubricant-impregnated thermosyphon. International Journal of Heat and Mass Transfer 2021;181:121871. https://doi.org/10.1016/j.ijheatmasstransfer.2021.121871.
[46] Preston DJ, Lu Z, Song Y, Zhao Y, Wilke KL, Antao DS, et al. Heat Transfer Enhancement During Water and Hydrocarbon Condensation on Lubricant Infused Surfaces. Scientific Reports 2018;8. https://doi.org/10.1038/s41598-017-18955-x.
[47] Ho JY, Rabbi KF, Sett S, Wong TN, Miljkovic N. Dropwise condensation of low surface tension fluids on lubricant-infused surfaces: Droplet size distribution and heat transfer. International Journal of Heat and Mass Transfer 2021;172:121149. https://doi.org/10.1016/j.ijheatmasstransfer.2021.121149.
[48] Sett S, Sokalski P, Mehta M, Rabbi KF, Gunay A, Miljkovic N. Transient pulse condensation. Appl Phys Lett 2020;117:091602. https://doi.org/10.1063/5.0015311.
[49] Eslami F, Elliott JAW. Thermodynamic Investigation of the Barrier for Heterogeneous Nucleation on a Fluid Surface in Comparison with a Rigid Surface. The Journal of Physical Chemistry B 2011;115:10646–53. https://doi.org/10.1021/jp202018e.
[50] Che Q, Lu Y, Wang F, Zhao X. Effect of substrate wettability and flexibility on the initial stage of water vapor condensation. Soft Matter 2019;15:10055–64. https://doi.org/10.1039/C9SM01783F.
[51] Guo L, Tang GH, Kumar S. Dynamic Wettability on the Lubricant-Impregnated Surface: From Nucleation to Growth and Coalescence. ACS Appl Mater Interfaces 2020;12:26555–65. https://doi.org/10.1021/acsami.0c03018.
[52] Sharma CS, Milionis A, Naga A, Lam CWE, Rodriguez G, Del Ponte MF, et al. Enhanced Condensation on Soft Materials through Bulk Lubricant Infusion. Adv Funct Materials 2021:2109633. https://doi.org/10.1002/adfm.202109633.
[53] Clanet C, Quéré D. Onset of menisci. J Fluid Mech 2002;460:131–49. https://doi.org/10.1017/S002211200200808X.
[54] Sun J, Weisensee PB. Microdroplet self-propulsion during dropwise condensation on lubricant-infused surfaces. Soft Matter 2019;15:4808–17. https://doi.org/10.1039/C9SM00493A.
[55] Guo Z, Zhang L, Monga D, Stone HA, Dai X. Hydrophilic slippery surface enabled coarsening effect for rapid water harvesting. Cell Reports Physical Science 2021;2:100387. https://doi.org/10.1016/j.xcrp.2021.100387.
[56] Sun J, Jiang X, Weisensee PB. Enhanced Water Nucleation and Growth Based on Microdroplet Mobility on Lubricant-Infused Surfaces. Langmuir 2021;37:12790–801. https://doi.org/10.1021/acs.langmuir.1c01559.
[57] Ge Q, Raza A, Li H, Sett S, Miljkovic N, Zhang T. Condensation of Satellite Droplets on Lubricant-Cloaked Droplets. ACS Appl Mater Interfaces 2020;12:22246–55. https://doi.org/10.1021/acsami.9b22417.
[58] Sun J, Weisensee PB. Marangoni-induced reversal of meniscus-climbing microdroplets. Soft Matter 2023;19:625–33. https://doi.org/10.1039/D2SM00979J.
[59] Zhu J-L, Shi W-Y, Wang T-S, Feng L. Spontaneous thermocapillary motion of condensation droplets. Appl Phys Lett 2020;116:243703. https://doi.org/10.1063/5.0007074.

[60] Teshima H, Misra S, Takahashi K, Mitra SK. Precursor-Film-Mediated Thermocapillary Motion of Low-Surface-Tension Microdroplets. Langmuir 2020;36:5096–105. https://doi.org/10.1021/acs.langmuir.0c00148.
[61] Lv F, Zhao F, Cheng D, Dong Z, Jia H, Xiao X, et al. Bioinspired functional SLIPSs and wettability gradient surfaces and their synergistic cooperation and opportunities for enhanced condensate and fluid transport. Advances in Colloid and Interface Science 2022;299:102564. https://doi.org/10.1016/j.cis.2021.102564.
[62] Laney SK, Michalska M, Li T, Ramirez FV, Portnoi M, Oh J, et al. Delayed Lubricant Depletion of Slippery Liquid Infused Porous Surfaces Using Precision Nanostructures. Langmuir 2021;37:10071–8. https://doi.org/10.1021/acs.langmuir.1c01310.
[63] Baumli P, D'Acunzi M, Hegner KI, Naga A, Wong WSY, Butt H-J, et al. The challenge of lubricant-replenishment on lubricant-impregnated surfaces. Advances in Colloid and Interface Science 2021;287:102329. https://doi.org/10.1016/j.cis.2020.102329.
[64] Kreder MJ, Daniel D, Tetreault A, Cao Z, Lemaire B, Timonen JVI, et al. Film Dynamics and Lubricant Depletion by Droplets Moving on Lubricated Surfaces. Phys Rev X 2018;8:031053. https://doi.org/10.1103/PhysRevX.8.031053.
[65] Peppou-Chapman S, Neto C. Depletion of the Lubricant from Lubricant-Infused Surfaces due to an Air/Water Interface. Langmuir 2021;37:3025–37. https://doi.org/10.1021/acs.langmuir.0c02858.
[66] Peppou-Chapman S, Neto C. Mapping Depletion of Lubricant Films on Antibiofouling Wrinkled Slippery Surfaces. ACS Applied Materials & Interfaces 2018;10:33669–77. https://doi.org/10.1021/acsami.8b11768.
[67] Hoque MJ, Sett S, Yan X, Liu D, Rabbi KF, Qiu H, et al. Life Span of Slippery Lubricant Infused Surfaces. ACS Appl Mater Interfaces 2022;14:4598–611. https://doi.org/10.1021/acsami.1c17010.
[68] Adera S, Alvarenga J, Shneidman AV, Zhang CT, Davitt A, Aizenberg J. Depletion of Lubricant from Nanostructured Oil-Infused Surfaces by Pendant Condensate Droplets. ACS Nano 2020;14:8024–35. https://doi.org/10.1021/acsnano.9b10184.
[69] Wang R, Jakhar K, Ahmed S, Antao DS. Elucidating the Mechanism of Condensation-Mediated Degradation of Organofunctional Silane Self-Assembled Monolayer Coatings. ACS Appl Mater Interfaces 2021;13:34923–34. https://doi.org/10.1021/acsami.1c08496.
[70] Ma J, Sett S, Cha H, Yan X, Miljkovic N. Recent developments, challenges, and pathways to stable dropwise condensation: A perspective. Appl Phys Lett 2020;116:260501. https://doi.org/10.1063/5.0011642.
[71] Tripathy A, Regulagadda K, Lam CWE, Donati MA, Milionis A, Sharma CS, et al. Ultrathin Durable Organic Hydrophobic Coatings Enhancing Dropwise Condensation Heat Transfer. Langmuir 2022;38:11296–303. https://doi.org/10.1021/acs.langmuir.2c01477.
[72] Zeng Q, Zhou H, Huang J, Guo Z. Review on the recent development of durable superhydrophobic materials for practical applications. Nanoscale 2021;13:11734–64. https://doi.org/10.1039/D1NR01936H.
[73] Scarratt LRJ, Steiner U, Neto C. A review on the mechanical and thermodynamic robustness of superhydrophobic surfaces. Advances in Colloid and Interface Science 2017;246:133–52. https://doi.org/10.1016/j.cis.2017.05.018.
[74] Mariam Varughese S, Bhandaru N. Durability of submerged hydrophobic surfaces. Soft Matter 2020;16:1692–701. https://doi.org/10.1039/C9SM01942A.
[75] Ma J, Cha H, Kim M, Cahill DG, Miljkovic N. Condensation Induced Delamination of Nanoscale Hydrophobic Films. Adv Funct Mater 2019;29:1905222. https://doi.org/10.1002/adfm.201905222.
[76] Berkelaar RP, Bampoulis P, Dietrich E, Jansen HP, Zhang X, Kooij ES, et al. Water-Induced Blister Formation in a Thin Film Polymer. Langmuir 2015;31:1017–25. https://doi.org/10.1021/la504002w.

[77] Wang R, Guo J, Muckleroy EA, Antao DS. Robust silane self-assembled monolayer coatings on plasma-engineered copper surfaces promoting dropwise condensation. International Journal of Heat and Mass Transfer 2022;194:123028. https://doi.org/10.1016/j.ijheatmasstransfer.2022.123028.
[78] Ma J, Zheng Z, Hoque MJ, Li L, Rabbi KF, Ho JY, et al. A Lipid-Inspired Highly Adhesive Interface for Durable Superhydrophobicity in Wet Environments and Stable Jumping Droplet Condensation. ACS Nano 2022;16:4251–62. https://doi.org/10.1021/acsnano.1c10250.
[79] Wilke KL, Antao DS, Cruz S, Iwata R, Zhao Y, Leroy A, et al. Polymer Infused Porous Surfaces for Robust, Thermally Conductive, Self-Healing Coatings for Dropwise Condensation. ACS Nano 2020;14:14878–86. https://doi.org/10.1021/acsnano.0c03961.
[80] Huang C, Qian X, Yang R. Thermal conductivity of polymers and polymer nanocomposites. Materials Science and Engineering: R: Reports 2018;132:1–22. https://doi.org/10.1016/j.mser.2018.06.002.
[81] Chang HC, Rajagopal MC, Hoque MJ, Oh J, Li L, Li J, et al. Composite Structured Surfaces for Durable Dropwise Condensation. International Journal of Heat and Mass Transfer 2020;156:119890. https://doi.org/10.1016/j.ijheatmasstransfer.2020.119890.
[82] Mondal B, Mac Giolla Eain M, Xu Q, Egan VM, Punch J, Lyons AM. Design and Fabrication of a Hybrid Superhydrophobic–Hydrophilic Surface That Exhibits Stable Dropwise Condensation. ACS Appl Mater Interfaces 2015;7:23575–88. https://doi.org/10.1021/acsami.5b06759.
[83] Hatte S, Stoddard R, Pitchumani R. Novel solid-infused durable nonwetting surfaces for sustained condensation heat transfer enhancement. Applied Thermal Engineering 2023;219:119458. https://doi.org/10.1016/j.applthermaleng.2022.119458.
[84] Xie J, Xu J, Li X, Liu H. Dropwise condensation on superhydrophobic nanostructure surface, Part I: Long-term operation and nanostructure failure. International Journal of Heat and Mass Transfer 2019;129:86–95. https://doi.org/10.1016/j.ijheatmasstransfer.2018.09.100.
[85] Dorrer C, Rühe J. Condensation and Wetting Transitions on Microstructured Ultrahydrophobic Surfaces. Langmuir 2007;23:3820–4. https://doi.org/10.1021/la063130f.
[86] Tang Y, Yang X, Li Y, Lu Y, Zhu D. Robust Micro-Nanostructured Superhydrophobic Surfaces for Long-Term Dropwise Condensation. Nano Lett 2021;21:9824–33. https://doi.org/10.1021/acs.nanolett.1c01584.
[87] Song J, Hou Y, Sudersan P, Lam CWE, Poulikakos D, Butt H-J, et al. Inhibition of condensation-induced droplet wetting by nano-hierarchical surfaces. Chemical Engineering Journal 2023;460:141761. https://doi.org/10.1016/j.cej.2023.141761.
[88] Stendardo L, Milionis A, Kokkoris G, Stamatopoulos C, Sharma CS, Kumar R, et al. Out-of-Plane Biphilic Surface Structuring for Enhanced Capillary-Driven Dropwise Condensation. Langmuir 2023;39:1585–92. https://doi.org/10.1021/acs.langmuir.2c03029.
[89] Yan X, Qin Y, Chen F, Zhao G, Sett S, Hoque MJ, et al. Laplace Pressure Driven Single-Droplet Jumping on Structured Surfaces. ACS Nano 2020;14:12796–809. https://doi.org/10.1021/acsnano.0c03487.
[90] Huang Y, Hu L, Chen W, Fu X, Ruan X, Xie H. Directional Transport of a Liquid Drop between Parallel–Nonparallel Combinative Plates. Langmuir 2018;34:4484–93. https://doi.org/10.1021/acs.langmuir.8b00172.
[91] Wisdom KM, Watson JA, Qu X, Liu F, Watson GS, Chen C-H. Self-cleaning of superhydrophobic surfaces by self-propelled jumping condensate. Proc Natl Acad Sci USA 2013;110:7992–7. https://doi.org/10.1073/pnas.1210770110.
[92] Lecointre P, Laney S, Michalska M, Li T, Tanguy A, Papakonstantinou I, et al. Unique and universal dew-repellency of nanocones. Nat Commun 2021;12:3458. https://doi.org/10.1038/s41467-021-23708-6.

[93] Mouterde T, Lehoucq G, Xavier S, Checco A, Black CT, Rahman A, et al. Antifogging abilities of model nanotextures. Nature Mater 2017;16:658–63. https://doi.org/10.1038/nmat4868.
[94] Zhang B, Chen X, Dobnikar J, Wang Z, Zhang X. Spontaneous Wenzel to Cassie dewetting transition on structured surfaces. Phys Rev Fluids 2016;1:073904. https://doi.org/10.1103/PhysRevFluids.1.073904.
[95] Sharma CS, Stamatopoulos C, Suter R, von Rohr PR, Poulikakos D. Rationally 3D-Textured Copper Surfaces for Laplace Pressure Imbalance-Induced Enhancement in Dropwise Condensation. ACS Appl Mater Interfaces 2018;10:29127–35. https://doi.org/10.1021/acsami.8b09067.
[96] Verho T, Korhonen JT, Sainiemi L, Jokinen V, Bower C, Franze K, et al. Reversible switching between superhydrophobic states on a hierarchically structured surface. Proc Natl Acad Sci USA 2012;109:10210–3. https://doi.org/10.1073/pnas.1204328109.
[97] Tang G, Niu D, Guo L, Xu J. Failure and Recovery of Droplet Nucleation and Growth on Damaged Nanostructures: A Molecular Dynamics Study. Langmuir 2020;36:13716–24. https://doi.org/10.1021/acs.langmuir.0c02809.
[98] Wang R, Wu F, Xing D, Yu F, Gao X. Density Maximization of One-Step Electrodeposited Copper Nanocones and Dropwise Condensation Heat-Transfer Performance Evaluation. ACS Appl Mater Interfaces 2020;12:24512–20. https://doi.org/10.1021/acsami.0c05224.
[99] Bintein P-B, Lhuissier H, Mongruel A, Royon L, Beysens D. Grooves Accelerate Dew Shedding. Phys Rev Lett 2019;122:098005. https://doi.org/10.1103/PhysRevLett.122.098005.
[100] Dong J, Dong H, Jin Y, Sun L, Ye S. Nanograssed Micro-V-Groove Architectures for Continuous Dropwise Condensation and Droplet Directional Movement. Advanced Materials Interfaces 2018;5:1800202. https://doi.org/10.1002/admi.201800202.
[101] Stamatopoulos C, Milionis A, Ackerl N, Donati M, Leudet de la Vallée P, Rudolf von Rohr P, et al. Droplet Self-Propulsion on Superhydrophobic Microtracks. ACS Nano 2020;14:12895–904. https://doi.org/10.1021/acsnano.0c03849.
[102] Wan Y, Sun K, Xu J, Yu H. Efficient removal of condensate droplets from the surface with microgroove composite structures. J Micromech Microeng 2023;33:035009. https://doi.org/10.1088/1361-6439/acb5ff.
[103] Ma C, Chen L, Wang L, Tong W, Chu C, Yuan Z, et al. Condensation droplet sieve. Nat Commun 2022;13:5381. https://doi.org/10.1038/s41467-022-32873-1.
[104] Shan L, Guo Z, Monga D, Boylan D, Dai X. Microchannel-elevated micromembrane for sustainable phase-separation condensation. Joule 2023;7:168–82. https://doi.org/10.1016/j.joule.2022.11.010.
[105] Zhang C, Wang D, Yang J, Zhang W, Sun Q, Yu F, et al. Charge Density Gradient Propelled Ultrafast Sweeping Removal of Dropwise Condensates. J Phys Chem B 2021;125:1936–43. https://doi.org/10.1021/acs.jpcb.0c10285.
[106] Oh I, Cha H, Chen J, Chavan S, Kong H, Miljkovic N, et al. Enhanced Condensation on Liquid-Infused Nanoporous Surfaces by Vibration-Assisted Droplet Sweeping. ACS Nano 2020;14:13367–79. https://doi.org/10.1021/acsnano.0c05223.
[107] Attinger D, Frankiewicz C, Betz AR, Schutzius TM, Ganguly R, Das A, et al. Surface engineering for phase change heat transfer: A review. MRS Energy & Sustainability 2014;1:4. https://doi.org/10.1557/mre.2014.9.
[108] Chehrghani MM, Abbasiasl T, Sadaghiani AK, Koşar A. Biphilic Surfaces with Optimum Hydrophobic Islands on a Superhydrophobic Background for Dropwise Flow Condensation. Langmuir 2021;37:13567–75. https://doi.org/10.1021/acs.langmuir.1c01844.
[109] Han T, Choi Y, Na KM, Kim MH, Jo H. Enhanced condensation on a biphilic-zigzag surface due to self-arrangement of crystals on a micro-structured surface. International Journal of Heat and Mass Transfer 2021;179:121710. https://doi.org/10.1016/j.ijheatmasstransfer.2021.121710.

[110] Mohamed MA, Ahmed SA, Emeara MS, Mesalhy O, Saleh MA. Experimental study for enhancing condensation on large-scale surface using hybrid hydrophilic-hydrophobic patterns. Case Studies in Thermal Engineering 2023;45:102984. https://doi.org/10.1016/j.csite.2023.102984.
[111] Boylan D, Monga D, Shan L, Guo Z, Dai X. Pushing the Limit of Beetle-Inspired Condensation on Biphilic Quasi-Liquid Surfaces. Advanced Functional Materials 2023;33:2211113. https://doi.org/10.1002/adfm.202211113.
[112] Zhu Y, Ho TC, Lee HH, Leung MKH, Tso CY. Droplet jumping physics on biphilic surfaces with different nanostructures and surface orientations under various air pressure conditions. Cell Reports Physical Science 2022;3:100849. https://doi.org/10.1016/j.xcrp.2022.100849.
[113] Wu S, Gao S, Wang H, Deng Z. Dropwise condensation heat transfer on vertical superhydrophobic surfaces with gradient microgrooves in humid air. International Journal of Heat and Mass Transfer 2023;201:123583. https://doi.org/10.1016/j.ijheatmasstransfer.2022.123583.
[114] Chen J, Dong K, He S, Deng W, Zhao J. Investigation of biphilic microgroove surface on condensation Enhancement: A 3D Lattice Boltzmann method study. Applied Thermal Engineering 2023;219:119520. https://doi.org/10.1016/j.applthermaleng.2022.119520.
[115] Abbasiasl T, Chehrghani MM, Sadaghiani AK, Koşar A. Gradient mixed wettability surfaces for enhancing heat transfer in dropwise flow condensation. International Journal of Heat and Mass Transfer 2021;179:121664. https://doi.org/10.1016/j.ijheatmasstransfer.2021.121664.
[116] Winter RL, McCarthy M. Dewetting from Amphiphilic Minichannel Surfaces during Condensation. ACS Appl Mater Interfaces 2020;12:7815–25. https://doi.org/10.1021/acsami.9b21265.
[117] Stetten AZ, Golovko DS, Weber SAL, Butt H-J. Slide electrification: charging of surfaces by moving water drops. Soft Matter 2019;15:8667–79. https://doi.org/10.1039/C9SM01348B.
[118] Li X, Bista P, Stetten AZ, Bonart H, Schür MT, Hardt S, et al. Spontaneous charging affects the motion of sliding drops. Nat Phys 2022. https://doi.org/10.1038/s41567-022-01563-6.
[119] Miljkovic N, Preston DJ, Enright R, Wang EN. Electrostatic charging of jumping droplets. Nat Commun 2013;4:2517. https://doi.org/10.1038/ncomms3517.
[120] Miljkovic N, Preston DJ, Enright R, Wang EN. Electric-Field-Enhanced Condensation on Superhydrophobic Nanostructured Surfaces. ACS Nano 2013;7:11043–54. https://doi.org/10.1021/nn404707j.
[121] Wang P, Min B, Wei L, Chen X, Wang Z, Chen Z, et al. Controlling the condensation of vapor by electric field: A molecular dynamics simulation study. Applied Surface Science 2022;605:154805. https://doi.org/10.1016/j.apsusc.2022.154805.
[122] Wang S-Y, Wang Z-J, Wang D-Q, Yang Y-R, Wang X-D, Lee D-J. Electrically Manipulated Vapor Condensation on the Dimpled Surface: Insights from Molecular Dynamics Simulations. Langmuir 2023;39:829–40. https://doi.org/10.1021/acs.langmuir.2c02897.
[123] Högnadóttir S, Kristinsson K, Thormar HG, Leosson K. Increased droplet coalescence using electrowetting on dielectric (EWOD). Appl Phys Lett 2020;116:073702. https://doi.org/10.1063/1.5140202.
[124] Hoek H, Dey R, Mugele F. Electrowetting-Controlled Dropwise Condensation with Patterned Electrodes: Physical Principles, Modeling, and Application Perspectives. Adv Mater Interfaces 2021;8:2001317. https://doi.org/10.1002/admi.202001317.
[125] Wikramanayake ED, Perry J, Bahadur V. AC electrowetting promoted droplet shedding on hydrophobic surfaces. Appl Phys Lett 2020;116:193701. https://doi.org/10.1063/5.0006117.
[126] Liu X, Cheng P. Dropwise condensation theory revisited Part II. Droplet nucleation density and condensation heat flux. International Journal of Heat and Mass Transfer 2015;83:842–9. https://doi.org/10.1016/j.ijheatmasstransfer.2014.11.008.
[127] Cho HJ, Preston DJ, Zhu Y, Wang EN. Nanoengineered materials for liquid–vapour phase-change heat transfer. Nat Rev Mater 2017;2:16092. https://doi.org/10.1038/natrevmats.2016.92.

[128] Donati M, Lam CWE, Milionis A, Sharma CS, Tripathy A, Zendeli A, et al. Sprayable Thin and Robust Carbon Nanofiber Composite Coating for Extreme Jumping Dropwise Condensation Performance. Adv Mater Interfaces 2021;8:2001176. https://doi.org/10.1002/admi.202001176.
[129] Ho JY, Rabbi KF, Khodakarami S, Sett S, Wong TN, Leong KC, et al. Ultrascalable Surface Structuring Strategy of Metal Additively Manufactured Materials for Enhanced Condensation. Advanced Science 2022;9:2104454. https://doi.org/10.1002/advs.202104454.
[130] Cha H, Wu A, Kim M-K, Saigusa K, Liu A, Miljkovic N. Nanoscale-Agglomerate-Mediated Heterogeneous Nucleation. Nano Lett 2017;17:7544–51. https://doi.org/10.1021/acs.nanolett.7b03479.
[131] Lavielle N, Beysens D, Mongruel A. Memory Re-Condensation. Langmuir 2023:acs.langmuir.2c03070. https://doi.org/10.1021/acs.langmuir.2c03070.
[132] Yu X, Dorao CA, Fernandino M. Droplet evaporation during dropwise condensation due to deposited volatile organic compounds. AIP Advances 2021;11:085202. https://doi.org/10.1063/5.0056005.
[133] Rose JW. Dropwise condensation theory and experiment: A review. Proceedings of the Institution of Mechanical Engineers, Part A: Journal of Power and Energy 2002;216:115–28. https://doi.org/10.1243/09576500260049034.
[134] Preston DJ, Mafra DL, Miljkovic N, Kong J, Wang EN. Scalable Graphene Coatings for Enhanced Condensation Heat Transfer. Nano Lett 2015;15:2902–9. https://doi.org/10.1021/nl504628s.
[135] Tenn FG, Missen RW. A study of the condensation of binary vapors of miscible liquids: Part I: The equilibrium relations. Can J Chem Eng 1963;41:12–4. https://doi.org/10.1002/cjce.5450410105.
[136] Ford JD, Missen RW. On the conditions for stability of falling films subject to surface tension disturbances; the condensation of binary vapors. The Canadian Journal of Chemical Engineering 1968;46:309–12.
[137] Zhang L, Iwata R, Zhao L, Gong S, Lu Z, Xu Z, et al. Nucleation Site Distribution Probed by Phase-Enhanced Environmental Scanning Electron Microscopy. Cell Reports Physical Science 2020;1:100262. https://doi.org/10.1016/j.xcrp.2020.100262.
[138] Wang Y, Rastogi D, Malek K, Sun J, Asa-Awuku A, Woehl TJ. Electric Field-Induced Water Condensation Visualized by Vapor-Phase Transmission Electron Microscopy. J Phys Chem A 2023;127:2545–53. https://doi.org/10.1021/acs.jpca.2c08187.
[139] Sijs R, Kooij S, Holterman HJ, Van De Zande J, Bonn D. Drop size measurement techniques for sprays: Comparison of image analysis, phase Doppler particle analysis, and laser diffraction. AIP Advances 2021;11:015315. https://doi.org/10.1063/5.0018667.
[140] Zhang L, Xu Z, Lu Z, Du J, Wang EN. Size distribution theory for jumping-droplet condensation. Applied Physics Letters 2019;114:163701. https://doi.org/10.1063/1.5081053.
[141] Weisensee PB, Wang Y, Hongliang Q, Schultz D, King WP, Miljkovic N. Condensate droplet size distribution on lubricant-infused surfaces. International Journal of Heat and Mass Transfer 2017;109:187–99. https://doi.org/10.1016/j.ijheatmasstransfer.2017.01.119.
[142] Guo Z, Monga D, Shan L, Boylan D, Dai X. Coarsening-induced disappearing droplets contribute to condensation. Droplet 2022;1:170–81. https://doi.org/10.1002/dro2.23.
[143] Suh Y, Lee J, Simadiris P, Yan X, Sett S, Li L, et al. A Deep Learning Perspective on Dropwise Condensation. Advanced Science 2021;8:2101794. https://doi.org/10.1002/advs.202101794.
[144] Khodakarami S, Fazle Rabbi K, Suh Y, Won Y, Miljkovic N. Machine learning enabled condensation heat transfer measurement. International Journal of Heat and Mass Transfer 2022;194:123016. https://doi.org/10.1016/j.ijheatmasstransfer.2022.123016.
[145] Wong HY, Wong LW, Tsang CS, Yan Z, Zhang X, Zhao J, et al. Superhydrophobic Surface Designing for Efficient Atmospheric Water Harvesting Aided by Intelligent Computer Vision. ACS Appl Mater Interfaces 2023;15:25849–59. https://doi.org/10.1021/acsami.3c03436.

[146] Hughes MT, Kini G, Garimella S. Status, Challenges, and Potential for Machine Learning in Understanding and Applying Heat Transfer Phenomena. Journal of Heat Transfer 2021;143. https://doi.org/10.1115/1.4052510.